



Conference Series 17

1st International Conference on Subduction, Volcanism and the Evolution of Oceanic and Continental Crust (SVEOCC 2014)

Abstract Volume

Editor

Holger Sommer

*Department of Geography, Earth Science and Environment,
University of the South Pacific, Fiji.*



School of Geography, Earth Science
and Environment

Organized by

**Department of Geography, Earth Science and Environment,
University of the South Pacific, Fiji.**

10-16 Februar, 2014

International Association for Gondwana Research Conference Series 17

1st International Conference on Subduction, Volcanism and the Evolution of Oceanic and Continental Crust (SVEOCC 2014), 10-16 February 2014, Nadi, Fiji.

Abstract Volume

Editor

Holger Sommer
Department of Geography, Earth Science and Environment,
University of the South Pacific, Fiji.

Published by the International Association for Gondwana Research
Headquarters: Journal Center, China University of Geosciences Beijing,
No. 29 Xueyuan Road, Haidian District, Beijing 100083, China
Pages: 66

© 2014, International Association for Gondwana Research

Contents

The global Moho depth map for continental crust <i>A. Baranov, A. Morelli.....</i>	7
Surface displacements, deformations and gravity changes due to underground heat source <i>L. Brimich, I. Kohút, P. Vajda.....</i>	9
Cretaceous transition from back-arc to foreland basin development in the northeastern Asian continental margin: Sedimentary and structural records from NE China <i>H. L. Chen, F. Q. Zhang, S. F. Yang, D. X. Chen, M. Na. A, T. Y. Shao, K. F. Zhang, B. Deng, G. E. Batt, Q. A. Meng, J. P. Liang, Z. Z. Wang....</i>	10
Phanerozoic Continental Growth in Asia and The “Cimmerian Orogeny” in Tethys <i>S. L. Chung, H. Y. Chiu, H. Y. Lee, F. Y. Wu, M. H. Zarrinkoub, A. Okrostsvaridze, G. Galoyan, A. F. Bingol.....</i>	11
Study on shoshonitic series, adakites and porphyry Cu-Au deposits in the Luzong volcanic basin: A clue to ridge subduction <i>J. Deng, X. Yang, W. Sun.....</i>	13
Direct dating of tsunami boulders: a 1500-year history of tsunami from the Suva lagoon, Fiji <i>S.J. Gale, K.K. Lal.....</i>	16
Is the Southwest Pacific a suitable analogue for the Central Asian Orogenic Belt and the Tasmanides of eastern Australia? <i>R. A. Glen.....</i>	17
Hydration of Archean lithosphere: A chemico-physical case study of the Iherzolitic upper mantle below the Kaapvaal Craton <i>J. Globig, H. Sommer, C. Gauert.....</i>	20
Al-spinel as Fe carrier during serpentinization <i>R. Huang, W. Sun.....</i>	21
Advances in finite-frequency inverse scattering and tomography using teleseismic data <i>M.V. de Hoop, S. Burdick, X. Shang, R.D. van der Hilst.....</i>	22

III-posed problem of regional modeling and major geodynamic periodicity <i>V.D. Kotelkin.....</i>	23
The late Mesoproterozoic to late Palaeozoic evolution of Central Asia and comparison with the SW Pacific <i>A. Kröner, Y. Rojas-Agramonte.....</i>	25
Seismic Evidence for Ancient Subduction of Izanagi Plate: Implications for Regional Mantle Viscosity <i>J. Li, D. A. Yuen.....</i>	27
Earthquakes, fluids, and climate - or: what controls orogeny in a forearc system? <i>O. Oncken.....</i>	31
The role of Serpentinite in lubricating Subduction Zones <i>T. Poulet, M. Veveakis, K. Regenauer-Lieb, D. A. Yuen.....</i>	33
Geology and setting of Viti Levu Island, Fiji <i>B. Rao.....</i>	34
Creep Fractures in the Mantle and their role for Deep Fluid Transfer <i>K. Regenauer-Lieb, M. Veveakis, T. Poulet, H. Sommer, A. Karrech, J. Liu, C. Schrank.....</i>	35
The formation of micro diamonds in decompression cracks out of equilibrium controlled by the C:O:H ratio in the kimberlitic melt <i>H. Sommer, B. Gasharova, K. Regenauer-Lieb, W. Colliston, J. Potgieter.....</i>	37
Petrography, petrology and mineralogy of eclogite nodules from the Jwaneng Diamond Mine, Botswana. An approach documented by mantle metasomatism, kimberlite emplacement and finally by super sonic uplift of the diamondiferous host rocks <i>H. Sommer, K. Regenauer-Lieb, O. Gaede, B. Gasharova.....</i>	38
From Gabbro to Granulite and finally to Kyanite- and bimineralic Eclogite: A petrological, geochemical and mass balance approach <i>H. Sommer, D. Jacob.....</i>	40
GPS Approach Detecting Tsunami Energy Scales in Real-Time for Early Warnings <i>Y. T. Song.....</i>	42
Multi-decadal regional sea level shifts in the Pacific over 1985-2008 <i>Y. T. Song, J. H. Moon.....</i>	43

Late Mesozoic Evolution of the back-arc basins of the Southeast China Block <i>L. Shu, J. Yao</i>	44
Basement nature of the Chinese and Mogolian Altai: Precambrian detrital zircons and interpretation <i>M. Sun, Y. Jiang, C. Yuan, G. Zhao, W. Xiao</i>	46
Porphyry deposits and oxidized magmas <i>W. Sun, H. Li, R. Huang, X. Ding, M. Ling</i>	47
Sea level trend in New Zealand over the last century <i>R. Tenzer, A. Fadil</i>	49
Signature of the ocean-floor spreading in marine gravity <i>R. Tenzer</i>	50
On capabilities of modern gravimetric methods in studying dynamic magmatic systems <i>P. Vajda, I. Prutkin, J. Gottsmann, M. Bielik, V. Bezák, R. Tenzer, L. Brimich</i>	51
Tectonic of accretionary wedges response to variation of incoming plate variations along Manila Trench <i>S. Wu, C. Chen</i>	55
Mesozoic subduction history of the Paleo-Pacific plate beneath the Eurasian continent: Evidence from volcanic rocks in NE China <i>W. Xu, F. Wang, F. P. Pei, H. Feng</i>	56
Changes in local weather after 2004 Indian Ocean tsunami <i>Z. Yan, D. Tang</i>	58
Neoproterozoic Pacific type trench-arc system in the Jiangnan Orogen belt, South China: some important traces from rock assemblages, zircon U-Pb dating, Hf isotopes and whole rock geochemistry <i>J. Yao, L. Shu</i>	59
Episodic widespread magma underplating in the Phanerozoic: Implication for craton destruction <i>H. F. Zhang</i>	61
Late Mesozoic giant magmatism in NE China and its adjacent region: Spatial-temporal variation and its tectonic significance <i>F. Q. Zhang, H. L. Chen, S. F. Yang, T. Y. Shao, M. N. A, K. F. Zhang, D. X. Chen, B. Deng, G. E. Batt, Q. A. Meng, J. P. Liang, Z. Z. Wang</i>	63

Jiangnan Orogen in South China: developed from divergent double
subduction?

Guochun Zhao.....65

The global Moho depth map for continental crust

A. Baranov^a, A. Morelli^b

^aSchmidt Institute of Physics of the Earth, Russian Academy of Sciences, Geodynamics, Moscow, Russian Federation

^bIstituto Nazionale di Geofisica e Vulcanologia, Sezione di Bologna, Italy
email: baranov@ifz.ru

Different tectonic units cover the continents: platform, orogens and depression structures. This structural variability is reflected both in thickness and physical properties of the crust. We present a new global Moho map for the continental crust, derived from geophysical data selected from the literature and regional crustal models. The Moho depth is represented with a resolution of 1×1 on a Cartesian grid. A large volume of new data has been analyzed: mostly active seismic experiments, as well as receiver functions and geological studies. We have used the following regional studies: for Europe, model EPcrust (Molinari and Morelli, 2011), for North Asia, Moho models from (Cherepanova et al., 2013; Iwasaki et al., 2013; Pavlenkova, 1996), for Central and Southern Asia, model AsCrust (Baranov, 2010), for Africa, the model by (Pasyanos and Nyblade, 2007) as a framework and added many others regional studies, for South America, models by (Assumpção et al., 2013; Chulick et al., 2013; Lloyd et al., 2010), for North America, the model by (Keller, 2013), for Australia, the model by (Salmon et al., 2013), for Greenland, data from (Dahl-Jensen et al., 2003) and others, for Antarctica, model

ANTMoho (Baranov and Morelli, 2013).

For two orogens we have found the maximum depth at – 75 km (Tibet and Andes). In our model the average thickness of the continental crust is about 34 km (st. deviation 9 km) whereas in CRUST 2.0 model average Moho for continental areas is about 38 km. The new Moho model for continents exhibits some remarkable disagreement at places with respect to global model CRUST 2.0. The difference in crustal thickness between these two models may amount up to 30 km, mainly due to improved resolution of our model's Moho boundary.

There are significant changes in several regions: among them, Darfur, Africa (–22 km); Madagascar (–28 / +14 km), Andes (–30 km); Parana delta, South America (–20 km); California (–20 km); Gamburtsev Mountains, East Antarctica (+24 km). Such analysis remains in large part true also for a comparison with Moho from recent CRUST 1.0 model, except a better agreement in the Americas.

Our model provides a starting point for numerical modeling of deep mantle structures via a thorough revision of the crustal effects in the observed fields. This model will be used as a starting

point in the gravity modeling of the lithosphere and upper mantle structures. Also it may be used for wave propagation modelling at continental scale, crustal correction in tomography and other seismological applications. The new model is available for download in digital format. We plan to update the model in the near future by including new data, particularly in the most poorly covered regions.

References

- Assumpção, M., Bianchi, M., Juliàc, J., Dias, F.L., França, G.S., Nascimento, R., Drouet, S., Pavão, C.S., Albuquerque, D.F., Afonso E.V. Lopes, A.E.V., 2013. Crustal thickness map of Brazil: Data compilation and main features. *Journal of South American Earth Sciences* 43, 74-85.
- Baranov, A., 2010. A New Model of the Earth's Crust in Central and South Asia. *Fiz. Zemli* 2010, 1, 37–50. *Izv. Phys. Earth (Engl. Transl.)*, 2010, 46, 1, 34–46.
- Baranov, A., Morelli, A., 2013. The Moho depth map of the Antarctica region. *Tectonophysics* 609, 299-313.
- Cherepanova, Y., Irina M. Artemieva, I.M., Thybo, H., Zurab Chemia, Z., 2013. Crustal structure of the Siberian craton and the West Siberian basin: An appraisal of existing seismic data. *Tectonophysics* 609, 154-183.
- Chulick, G.S., Detweiler, S., Mooney, W.D., 2013. Seismic structure of the crust and uppermost mantle of South America and surrounding oceanic basins. *Journal of South American Earth Sciences* 42, 260-276.
- Dahl-Jensen, T., Larsen, T.B., Ingo Woelbern, I., Bach, T., Hanka, W., Kind, R., Gregersen, S., Mosegaard, K., Voss, P., Gudmundsson, O., 2003. Depth to Moho in Greenland: receiver-function analysis suggests two Proterozoic blocks in Greenland. *Earth and Planetary Science Letters* 205, 379-393.
- Iwasaki, T., Levin, V., Nikulin, A., Iidaka, T., 2013. Constraints on the Moho in Japan and Kamchatka. *Tectonophysics* 609, 184-201. Keller, G.R., 2013. The Moho of North America: A brief review focused on recent studies. *Tectonophysics* 609, 45-55.
- Lloyd, S., van der Lee, S., França, G.S., Assumpção, M., Feng, M., 2010. Moho map of South America from receiver functions and surface waves. *Journal of Geophysical Research, Solid Earth* 115, 1-12.
- Molinari, I., Morelli, A., 2011. EPcrust: a reference crustal model for the European Plate. *Geophysical Journal International* 185, 352-364.
- Pasyanos, M.E., Nyblade, A.A., 2007. A top to bottom lithospheric study of Africa and Arabia. *Tectonophysics* 444, 27-44.
- Salmon, M., Kennett, B.L.N., Stern, T., Atiken, A.R.A., 2013. The Moho in Australia and New Zealand. *Tectonophysics* 609, 288-298.

Surface displacements, deformations and gravity changes due to underground heat source

L. Brimich, I. Kohút, P. Vajda

Geophysical Institute, Slovak Academy of Sciences, Dúbravská cesta 9, 842 28 Bratislava, Slovakia.
email: geofbrim@savba.sk

Thermo-elastic strains and stresses play a considerable role in the stress state of the lithosphere and its dynamics, especially at pronounced positive geothermal anomalies. Topography has a significant effect on ground deformation. Two methods for including the topographic effects in the thermo-viscoelastic model are described. First we use an approximate methodology, which assumes that the main effect of the topography is due to distance from the source to the free surface and permits to have an analytical solution very attractive for solving the inverse problem. A numerical solution (for 2D plain strain case) is also computed using finite element method (FEM). The numerical method allows include the local

shape of the topography in the modeling. In the numerical model the buried magmatic body is represented by a finite volume thermal source of variable power density. The temperature distribution is computed by the higher-degree FEM. For analytical as well as numerical model solution only the forces of thermal origin are considered. The results show that for the volcanic areas with an important relief the perturbation of the thermo-viscoelastic solution (deformation and total gravity anomaly) due to the topography can be quite significant. In consequence, neglecting topography could give erroneous results in the estimated source parameters.

Cretaceous transition from back-arc to foreland basin development in the northeastern Asian continental margin: Sedimentary and structural records from NE China

H-L. Chen^{a, b}, F-Q. Zhang^{a, b}, S-F. Yang^{a, b}, D-X. Chen^{a, b}, M-N. A^{a, b}, T-Y. Shao^{a, b}, K-F. Zhang^{a, b}, B. Deng^{a, b}, G. E. Batt^c, Q-A. Meng^d, J-P. Liang^d, Z-Z. Wang^d

^a Department of Earth Sciences, Zhejiang University, Hangzhou, China

^b Structural Research Center of Oil & Gas Bearing Basin of Ministry of Education, Hangzhou, China

^c The Centre for Exploration Targeting, University of Western Australia, Australia

^d Research Institute of Petroleum Exploration and Development, Daqing Oil Field, China

email: hlchen@zju.edu.cn

During the Cretaceous evolution of the northern East Asian continent, back-arc basin formation in an extensional setting was followed by foreland basin development in a compressional setting. Sedimentary and structural records of this tectonic transition are identified from the Songliao Basin and adjacent region in NE China. Early Cretaceous back-arc extension is featured by the development of numerous grabens and half-grabens, widespread silicic magmatism and synchronous exhumation of metamorphic core complex in the early stage, followed by development of several large terrestrial sags due to the thermal-cooling in the late stage. During the Late Cretaceous, compression was dominant in NE China and adjacent region. The northeastern Asian continental margin near the trench was featured by continental arc magmatism, metamorphism and rapid uplifting. A retroarc foreland basin system related to the paleo-Pacific subduction was identified toward the hinterland in NE China: the eastern Heilongjiang and Jilin assigned the fold-thrust belt roughly parallel the marginal

orogenic belt, the Songliao Basin assigned the elongate foredeep trough, the Great Xing'an Range assigned the forebulge, the Hailar and Erlian basins assigned the back-bulge sag in the latest stage. Changes in sediment dispersal patterns in the Songliao Basin, together with a following westward shift depocenter, record westward migration of the foreland basin system. This significant variation of the Cretaceous basin system in NE China is inferred to be the surface response of the tectonic transition from a Western Pacific-type to an Andean-type active margin, possibly resulting from the dip decrease of the Benioff subduction zone of paleo-Pacific plate along the northeastern Asian continental margin.

Acknowledgement

This work was financially supported by National Natural Science Foundation of China (Grant No. 41272231, 41330207) and the National Science and Technology Major Project Program of China (Grant No. 2011ZX05009-001).

Phanerozoic Continental Growth in Asia and The “Cimmerian Orogeny” in Tethys

S-L. Chung^a, H-Y. Chiu^a, H-Y. Lee^a, F-Y. Wu^b, M. H. Zarrinkoub^c, A. Okrostsvardze^d, G. Galoyan^e, A. F. Bingol^f

^aDepartment of Geosciences, National Taiwan University, Taipei, Taiwan

^bInstitute of Geology and Geophysics, Chinese Academy of Sciences, Beijing, China

^cDepartment of Geology, Birjand University, Birjand, Iran

^dInstitute of Earth Sciences, Ilia State University, Tbilisi, Georgia

^eInstitute of Geology, Armenian National Academy of Sciences, Yerevan, Armenia

^fDepartment of Geological Engineering, Firat University, Elazig, Turkey

Asia that comprises numerous ancient cratonic blocks and young mobile belts is the largest composite continent on Earth. It was enlarged by successive accretion of dispersed terranes that, associated with opening and closure of the Paleo-Asian and Tethys oceans, had produced a vast amount of juvenile continental crust. The Central Asian orogenic belt (CAOB), for instance, is celebrated for its accretionary tectonics and production of massive juvenile crust in the Phanerozoic or, most significantly, in the Paleozoic. The Tethyan domain consisted of two major oceans, i.e., Paleo-Tethys in north and Neo-Tethys in south, separated by a strip of continents/terrains called the Cimmerian Continent (Sengör, 1984), most of which had begun splitting from the northern margin of Gondwanaland during Triassic time. Elimination of the Tethyan oceans by collisions of the Cimmerian Continent and subsequent Gondwana-derived terrains with Eurasia resulted in a double, largely over-printed orogenic system, i.e., the Alpine-Himalayan orogenic belt. Here we synthesize zircon U-Pb and Hf

isotope data of magmatic rocks from West and South Asia, in particular from “CIA” (Caucasus/Iran/Anatolia) and Tibet, along the eastern Tethyan orogenic belt (ETOB) or eastern part of the typically collisional Alpine-Himalayan system. The data suggest that, before collisions started, the entire region was characterized not only by Tethyan subductions but also by accretionary orogenic processes that led to the formation of a vast amount of juvenile crust from the Jurassic to Eocene or, in places, to Oligocene. Taking together, both the CAOB and ETOB appear to have evolved through time from an accretionary into a collisional system. Zircon Hf isotope data further reveal that, in contrast to generating massive juvenile crust in the earlier, accretionary stages of orogenic development, crustal recycling plays a more substantial role in the subsequent, collisional stages. The latter involves addition of older continental crust into the mantle, which in turn melted and caused compositional transformation of the juvenile crust formed in the accretionary stages. Similar features are observed in young volcanic rocks from eastern

Taiwan, i.e., the northern Luzon arc and part of the complex subduction system in Southeast Asia, which may evolve one day to resemble the CAOB or ETOB by collision with the advancing Australian continent.

References

- Sengör, A.M.C., 1984. The Cimmeride Orogenic System and the Tectonics of Eurasia. Geological Society of America Special Papers 195, 1-74.

Study on shoshonitic series, adakites and porphyry Cu-Au deposits in the Luzong volcanic basin: A clue to ridge subduction

J. Deng^a, X. Yang^{a*}, W. Sun^b

^aCAS Key Laboratory of Crust-Mantle Materials and Environments, University of Science and Technology of China, Hefei 230026, China

^bCAS Key Laboratory of Isotope Geochronology and Geochemistry, Guangzhou Institute of Geochemistry, Chinese Academy of Sciences, Guangzhou 510640
email: xyyang555@163.com

The Luzong volcanic basin is in the north bank of the Yangtze River, located at the south margin of Yangtze and North China craton boundary, and eastern of the Tan-Lu fault. Magmatic rocks in the LYMB are mainly classified as three series: (1) a high-K calc-alkaline series, mainly developed in uplifted areas such as the Tongling and Anqing regions (Chang et al., 1991); (2) a Shoshonite series, normally formed in faulted volcanic basins represented by the Luzong and Nanjing-Wuhu areas (Ren et al., 1991; Wang et al., 1996); (3) A-type granitoids (alkaline intrusive rocks and granites), distributed along the Yangtze River fault, both in the uplift zones and fault zones (Xing and Xu, 1999). Yu and Bai (1981) first proposed the presence of a Mesozoic shoshonitic volcanic province in the Luzong region, with 70% of the surficial exposures as intermediate rocks and less than 30% as mafic rocks. Large-scale Fe-Cu-Au mineralization in the Luzong volcanic basin is associated with these igneous series (Ren et al., 1991; Chang et al., 1991; Yang 1996; Yang and Lee, 2005, 2011; Yang et al., 2001, 2002, 2005, 2011). Massive iron-sulfide mineralization and porphyry Cu-Au deposits occurred during the

magmatic activities in the Yanshanian period, forming series of large deposits, i.e., the Longqiao and Daobaozhuang Fe-S deposits; Shaxi porphyry Cu-Au deposits (Chang et al., 1991; Ren et al., 1991; Yang, 1996).

We studied on two types of Mesozoic magmatic rocks in Luzong volcanic basin, Nb-enriched shoshonites and adakites in Shaxi. The formation age of Shaxi adakites is 127.6-129.1 Ma, later than that of Luzong shoshonites. They have similar characteristics of major elements and show similar distribution pattern of trace elements (enriched in LILEs and depleted in HFSEs) and REEs (enriched in LREEs and depleted in HREEs, no Eu negative anomaly, flat HREEs pattern). Sr-Nd-Pb and Lu-Hf isotopic compositions of the two types of rocks show a few differences, exhibit MORB and subducting sediments in their source, distinct from adakites/granites derived from LCC of Yangtze craton. The shoshonites have high K₂O+Na₂O contents and K₂O/Na₂O ratios, high Nb contents and Nb/Ta ratio (14.99 av.) close to the value of subducting sediments (~14.2), varied Mg#, low Ce/Pb and Sr/La, low Ba/La and varied Th/Yb

suggesting an origin of subducting sediments with oceanic crust compositions. The adakites have high MgO contents, Mg#, Sr contents and S/Y ratios, low (La/Yb)_N, decoupling Sr/Y and (La/Yb)_N, exhibit of characteristics of slab melting derived adakites. The feature of low Sr/La, Th/Yb ratios and varied Ce/Pb, Ba/La ratios further supports that they are derived from partial melting of oceanic crust with subducting crust added, either. The combination of adakites and Nb-enriched shoshonites support a ridge subduction of paleo-pacific in the LYRB in Mesozoic, and it is probably the cause of large scale of Cu-Au mineralization in LYRB in Mesozoic.

We proposed fact that the assemblages of Nb-enriched shoshonites and adakites are typical combinations in the Luzong volcanic basin, their origins are related to the ridge subduction of paleo-pacific in Cretaceous. This subduction is probably the cause of large scale of Fe-Cu-Au mineralization in LYRB in Mesozoic. The sources of Nb-enriched shoshonites in Luzong are fluids/melts derived from partial melting of subduction sediments with oceanic crust. The mantle wedge metasomatized by the fluids/melts partial melted generated the Nb-enriched shoshonites from slab window. The Shaxi adakites are derived from partial melting of seawater altered oceanic crust added with subduction sediments.

Keywords Adakite; Nb-enriched shoshonite; geochemistry; slab melting; Ridge subduction; Luzong volcanic basin

References

- Chang, Y.F., Liu, X.P., Wu, Y.C., 1991. The Copper-Iron Belt of the Middle and Lower Reaches of the Changjiang River. Geological Publishing House, Beijing (in Chinese)
- Deng, J.H., Yang, X.Y., Sun, W.D., Huang, Y., Chi, Y.Y., Yu, L.F., Zhang, Q.M., 2012. Petrology, geochemistry, and tectonic significance of Mesozoic shoshonitic volcanic rocks, Luzong volcanic basin, eastern China. International Geology Review 54, 714-736.
- Li, 1994
- Ren, Q.J., Liu, X.S., Xu, Z.W., 1991. Luzong volcanic basin of Mesozoic era and the mineralization, Anhui, East China. Geological Publishing House, Beijing (in Chinese).
- Wang, D.Z., Ren, Q.J., Qiu, J.S., Chen, K.R., Xu, Z.W., Zen, J.H., 1996. Characteristics of volcanic rocks in the shoshonite province, eastern China and their metallogenesis. Acta Geologica Sinica 70, 23-34 (in Chinese with English abstract).
- Xing, F.M., Xu, X., 1999. Yangtze Magmatic Belt and Metallogenesis. Anhui People's Publishing House, Hefei. (in Chinese).
- Yang, X.Y., 1996. The Cu-Au metallogenic prospecting areas from middle-lower reaches of Changjiang River: A study on metallogenic geochemistry of some typical copper and gold ore deposits, Department of Earth

- and Space Sciences. University of Science and Technology of China, Hefei, pp. 1-214 (in Chinese with English abstract).
- Yang, X.Y., Lee, I.S., 2005. Geochemistry and metallogenesis in the lower part of the Yangtze metallogenic valley: A case study of the Shaxi-Changpushan porphyry Cu-Au deposit and a review of the adjacent Cu-Au deposits. *Neues Jahrbuch Fur Mineralogie-Abhandlungen* 181, 223-243.
- Yang, X.Y., Lee, I.S., 2011. Review of the stable isotope geochemistry of Mesozoic igneous rocks and Cu–Au deposits along the middle–lower Yangtze Metallogenic Belt, China. *International Geology Review* 53, 741-757.
- Yang, X.Y., Yang, X.M., Sun, L.G., Wang, K.R., 1998. Structural geochemistry and mineralization background and analyse of porphyric Cu(Au) deposit in Shaxi-Changpushan district. *Geology of Anhui* 8, 11-15 (in Chinese).
- Yang, X.Y., Yang, X.M., Zhang, Z.W., Chi, Y.Y., Yu, L.F., Zhang, Q.M., 2011a. A porphyritic copper (gold) ore-forming model for the Shaxi-Changpushan district. Lower Yangtze metallogenic belt, China: Geological and geochemical constraints. *International Geology Review* 53, 580-611.
- Yang, X.Y., Yang, X.M., Zhang, Z.W., Chi, Y.Y., Yu, L.F., Zhang, Q.M., 2011b. A porphyritic copper (gold) ore-forming model for the Shaxi-Changpushan district, Lower Yangtze metallogenic belt, China: geological and geochemical constraints. *International Geology Review* 53, 580-611.
- Yu, X.Y., Bai, Z.H., 1981. Trachyandesite Series in Luzong, Anhui. *Geochemica* 1, 57-65 (in Chinese with English abstract).
- Acknowledgement** The study is supported by the Natural Science Foundation of China (No.41173057 and 41372078).

Direct dating of tsunami boulders: a 1500-year history of tsunami from the Suva lagoon, Fiji

S.J. Gale, K.K. Lal

School of Geography, Earth Science and Environment, the University of the South Pacific, Suva, Fiji.

Sedimentary records of extreme wave events have been used to extend the historical record of tsunami and provide information on their frequency of occurrence and their potential environmental and human impact. For this project, $^{230}\text{Th}/^{234}\text{U}$ geochronometry was employed to determine the date at which coral growth in wave-transported coral blocks ceased, the date of detachment of the blocks from the living reef and thus the timing of tsunami wave impact.

Although sedimentary archives capable of preserving information on extreme wave events are not uncommon, distinguishing the depositional products of tsunami from those of other high-magnitude events such as tropical cyclones and extreme storms is far from straightforward.

Suva Lagoon on Viti Levu island, Fiji represents one of the few locations in the world where it is possible to assign an unequivocal tsunami origin to deposits laid down by extreme waves. We have exploited this potential to reconstruct a detailed and near-complete record of tsunami (and their causative submarine landslides and earthquakes) encompassing the last 1500 years. The average periodicity of damaging events is 300 years. This lies within human timescales and has important implications for hazard assessment and for efforts to minimise tsunami impact.

Is the Southwest Pacific a suitable analogue for the Central Asian Orogenic Belt and the Tasmanides of eastern Australia?

R. A. Glen

GEMOC, Department of Earth and Planetary Sciences, Macquarie University NSW 2109 AUSTRALIA,
email: geology.rg@gmail.com

The CAOB (Central Asian Orogenic Belt) and the Tasmanides of eastern Australia are two of Earth's great collages of non-collisional orogens. Convergence in the Central Asian Orogenic Belt, along its northern margin, commenced ~1000 Ma and ceased in the south either in the Carboniferous or mid-Permian to mid-Triassic (Xiao et al. 2009). The early history (~830-600 Ma) of the Tasmanides, in contrast, is one of rift basin formation consequent on the breakup of Rodinia, before localised convergent margin tectonism at ~590 Ma, and the onset of subduction along the Gondwana-Pacific plate boundary at 535-540 Ma. Convergent margin tectonism in the Tasmanides ceased at ~100 Ma, with the Cretaceous (rifted) arc best preserved along the east coast of Queensland (Whitsunday Islands). Magmatic roots are present in inland Queensland and especially as the Median Batholith of western and southern New Zealand.

The Southwest Pacific is an area ~2500 km east-west by ~4000 km north-south that comprises the submerged part of the Australian plate, which lies west and south of the modern Pacific plate. After (poorly defined) major plate boundary roll back of ~1500 km between ~100 and 55 Ma that

generated the Tasman and Coral seas, the Australian-Pacific plate boundary was re-established along the now extinct WNW-trending, SW-dipping Vitiaz Trench in the north and along a NNE-trending WNW-dipping trench in the south that subsequently rolled back with the opening of the South Fiji Basin from ~35 Ma to ~18 Ma.

Key tectonic elements of the Southwest Pacific consist of:

i) rifted-off continental ribbons such as the Lord Howe Rise and the Norfolk Ridge that are overlain by continental to marine sedimentary and volcanic rocks. The Norfolk Ridge includes New Caledonia, and extends south into Zealandia, encompassing New Zealand and flanking submarine continental shelves;

ii) a really dominant sedimentary basins that formed as backarc basins by rifting or by rifting leading to sea floor spreading behind either present day active arc segments (Tasman and Coral seas, Woodlark, North Fiji, Lau, Havre Trough) or inactive arc segments (North Loyalty, South Fiji, Norfolk Basin). Some basins like the New Caledonia might be composite (Cretaceous and Paleogene). Rift-related and or MORB-like volcanic and volcaniclastic rocks form the

ocean floors, in places interleaved with continentally-derived sediments .

iii) volumetrically minor intraoceanic arc systems. These include: a) modern plate boundary arcs. In the north this arc stretches from the Solomon Islands, (~7-0 Ma), southeast through Vanuatu (~7-0 Ma), to Fiji (~12-3 Ma), via the Hunter Ridge (~7-3 Ma). This arc developed upon the older Vitiaz arc in response to the initiation of east-dipping, plate boundary subduction after the Ontong Java collided with the Australian plate. In the south, west-dipping subduction of the Pacific plate beneath the Australian plate generated the Tofua (Tonga)-Kermadec arc (initiated at ~3.5 Ma above an older west-dipping supra-subduction zone system) and its southern extension, the 2-0 Ma Taupo Volcanic Zone of the North Island of New Zealand; b) rifted fragments of the older (Vitiaz) arc, which developed above the southwest dipping Vitiaz Trench after changes in plate boundary configurations following the ~ 44 Ma New Caledonia forearc-continent collision. Fragments of this arc occur in the Solomon Islands (~?62-24 Ma), Vanuatu (30-25 Ma), Fiji (>37-35 Ma). The Lau-Colville ridge (40-17 Ma) is a relict arc stranded after opening of the Lau Basin and the Havre Trough between it and the Tofua – Kermadec arc. Other older arcs occur on the Tonga ridge (46-17 Ma) and as the Northland arc in New Zealand (~23-20 Ma); c). relics of a ~23-18 Ma arc system, which stretches south from the

South d'Entrecasteaux Ridge, through the Loyalty Ridge into the Three Kings Ridge, the Northland Plateau and onto Northland in the North Island of New Zealand. This arc system is either intraplate, developed above an east-dipping subduction zone, or marks a west-dipping plate boundary that predates opening of the South Fiji Basin; d) old arcs in New Guinea at the northern margin of the Australian plate, such as the Papua (~70-65 Ma), Sepik (~49-37 Ma) and the Finisterre (~30-20 Ma) and accreted by oblique slip in the Paleocene, Oligocene and Miocene respectively; and e) local relics of older arc magmatism such as that at 55 Ma in New Caledonia.

iv) allochthons that consist either of complete sections through oceanic crust (Papuan Ultramafic Belt, and the peridotite belt of New Caledonia) or the upper part of ocean crust, preserved as the North Island Allochthon of New Zealand. The age of obduction youngs from north to south: 61-58 Ma for the Papuan Ultramafic Belt; 44-34 Ma for New Caledonia, ~38 Ma based on dredge hauls in the Three Kings Rise area and 25-22 Ma in New Zealand. There are two models for obduction south of New Caledonia: either continuation of the New Caledonia model, with a NE dipping slab upthrust as a result of microplate subduction and collision dipping to the NE; or rollback to the east of a single west-dipping plate boundary arc-trench system.

vi) hotspot magmatism such as in the Tasman Sea and Lord Howe Rise.

The paleogeography developed in Southwest Pacific region over the last ~100 million years has been used as a possible template for both the Central Asian Orogenic Belt and the Tasmanides. If a “forward modeled” Southwest Pacific paleogeography can be applied to these orogenic collages, what would it contain? Relics of old arcs (65-0 Ma), largely intermediate to mafic in composition, and intraoceanic rather than continental and felsic. Many such were built on even older arc systems. These relict island arcs would mainly mark the old plate boundary. They would probably not show any preferred younging direction, or even variable or even contradictory evidence of plate rollback or advance. There could be very little evidence of transfer of material across the old plate boundary, since almost all the shortening would have taken place in the largely submerged part of the ‘Australian’ plate as various parts became emergent. One would expect to find old internal continental blocks, and their deformed cover, flanked by collapsed backarc basins, both intruded by granitoids, with boundaries marked by newly formed (0 to -100Ma) intraplate arcs, subduction complexes obducted ocean crust and other evidence of arc-continent collisions.

Some of these features do not accord easily with key elements of the Tasmanides as deduced in a recent synthesis (Glen 2013), although from the mid-Silurian to the-end Carboniferous the Lachlan Orogen, and the poorly known Thomson Orogen to the north,

developed as marine then continental backarc basins behind a west-dipping plate boundary. Problematic features include the dominance of Ordovician quartz-rich, craton-derived turbidites; a single period of rollback, over 2000 km, from 520 to 500 Ma with a subsequent largely stationary plate boundary marked by a continental margin arcs; well-developed mid-Silurian to latest Carboniferous subduction complexes in the New England Orogen and no evidence for intraplate supra-subduction zone activity. With regard to the Central Asian Orogenic Belt, formation from a Southwest Pacific-type paleogeography implies the presence of arcs hundreds to thousands of kilometres long, and the dominance of deformed backarc basins rather than forearc basins or accretionary complexes.

References

- Glen, R. A., 2013. Refining accretionary orogen models for the Tasmanides of eastern Australia. *Australian Journal of Earth Sciences* 60, 315-370.
- Xiao, W. J., Windley, B. F., Huang, B. C., Han, C. M., Yuan, C., Chen, H. L., Sun, M., Sun, S., Li, J. L., 2009. End-Permian to mid-Triassic termination of the accretionary processes of the southern Altaids: implications for the geodynamic evolution, Phanerozoic continental growth, and metallogeny of Central Asia. *International Journal of Earth Sciences (Geologische Rundschau)* 98, 1189–1217.

Hydration of Archean lithosphere: A chemico-physical case study of the Iherzolitic upper mantle below the Kaapvaal Craton

J. Globig^a, H. Sommer^b, C. Gauert^c

^aGroup of Dynamics of the Lithosphere (G.D.L.), Institute of Earth Sciences Jaume Almera - CSIC, Spain

^bSchool of Geography, Earth Science and Environment, University of the Southern Pacific, Suva, Fiji

^cDept. of Geology, University of the Free State, P.O.Box 339, Bloemfontein 9300, R.S.A.; email: info@holgersommer.de

Since its formation in the Archean the subcratonic upper mantle of the Kaapvaal in southern Africa has undergone several processes of modification. Detailed analysis of Kaapvaal xenoliths from kimberlites show clear differences in age, origin, mineralogy, fertility and degree and type of alteration illustrating a period of complex interaction between asthenospheric and lithospheric mantle domains. The evolution of the cratonic lithosphere through time involved several metasomatic events leading to chemical and thermal anomalies. Global and regional 3-D shear wave velocity models are imaging a low velocity zone for the lower Kaapvaal lithosphere. However, regardless the resolution and significance of the lithospheric low velocity zone its origin is a matter of debate and is discussed to be either of thermal or chemical nature. Petrological evidences point to a rather chemical origin caused by refertilization and/or hydration of lithospheric mantle by metasomatizing fluids.

Here we present a chemico-physical study of the Iherzolitic lithosphere below South Africa using a recalculated bulk composition based on analyses of the rock forming minerals from Iherzolites from the Roberts Victor Mine. The thermo-chemical calculations were done for a water saturated Iherzolite representative of published compositions of garnet Iherzolites from the Kaapvaal Craton in order to estimate the distribution of hydrous phases and the combined influence on physical properties as density and P- and S-wave velocities. Our results confirm the existence of a zone with slightly lower S-wave velocities and are supporting the idea of chemically layered Iherzolitic mantle that has been repeatedly hydrated by slab released volatiles in a two sided subduction model.

Al-spinel as Fe carrier during serpentinization

R. Huang^{a, c}, W. Sun^{b*}

^aState Key Laboratory of Isotope Geochemistry, Guangzhou Institute of Geochemistry, Chinese Academy of Sciences, Guangzhou, 510640, China

^bCAS Key Laboratory of Mineralogy and Metallogeny, Guangzhou Institute of Geochemistry, Chinese Academy of Sciences, Guangzhou, 510640, China

^cUniversity of the Chinese Academy of Sciences, Beijing 100049, China

Although Al-spinel is a minor component of peridotite, it plays an important role during serpentinization. Experiments taking peridotite as starting material at 500-600 °C and 1-2 GPa show that spinel is altered to thick layers of ferrichromit and magnetite surrounding the unaltered spinel. However, only quite a few magnetite precipitates after complete alteration of orthopyroxene and almost no magnetite forms after alteration of olivine and clinopyroxene. Compare to experiments at 500-600 °C and 1-4 kbar that have much larger amounts of iron oxide, the major difference is that spinel at

500-600 °C and 1-4 kbar is altered to a thin layer of magnetite surrounding a large fraction of unaltered spinel. An experiment using crushed spinel as starting material at 500 °C and 3 kbar shows that spinel is not altered to magnetite-rich layer. Thus, the Fe forming magnetite layer at the edge of spinel is from fluid after alteration of olivine and pyroxene but not due to more depletion of Al, Mg, and Cr of spinel itself. We propose that spinel acts as Fe carrier during serpentinization, which “absorb” iron after alteration of olivine and pyroxene resulting in quite few amounts of magnetite formed after alteration of olivine and pyroxene.

Advances in finite-frequency inverse scattering and tomography using teleseismic data

M.V. de Hoop*, S. Burdick, X. Shang, R.D. van der Hilst

*Purdue University, 150 N. University Street, MATH Building, West Lafayette, USA

We present a framework of reverse-time continuation based inverse scattering and wave-equation tomography while invoking a separation of scales in the spatial variation of the elastic parameters describing Earth's interior. We give a generalization of receiver functions, which we refer to as array receiver functions, and develop a novel form of reflection tomography for teleseismic free-surface multiples. The growing availability of high-quality regional data inspires us to consider new phases that can aid us to better constrain seismic properties in the lithosphere and upper mantle. Teleseismic conversions and free-surface multiples are quite commonly being used to generate images of structures like the crust-mantle boundary (Moho)

and the lithosphere-asthenosphere boundary (LAB) but can also be used to image subducting slabs. Wave-equation reflection tomography provides information about the coarse scales or "background" model component through a measure of consistency (via a cross correlation power) of the images (obtained from single events) of the fine-scale model component. Using these reflected phases has the advantage of localizing velocity updates to the volumes above (or in between) the discontinuities, whereas teleseismic transmission tomography tends to have a very poor vertical resolution in the lithosphere. We briefly mention the use of ambient-noise generated data.

III-posed problem of regional modeling and major geodynamic periodicity

V.D. Kotelkin

Faculty of Mechanics and Mathematics of Lomonosov Moscow State University, Moscow, Russia

Appearance of detailed data about the internal structure of many regions of the Earth led to growth a new branch of geodynamic modeling - real regional modeling with using data from seismic tomography. The recent calculations of Ismail-Zadeh et al. (2013) are impressive example of such modeling. On the one hand such realistic simulation is very attractive, since it promises important forecasts, but on the other hand a new approach raises serious questions about the correctness of the simulation in the separate region. At first sight the use of real (ie correct) data should lead to correct results. However, mathematicians are well aware that in elliptic problems (geodynamics is such task) solution into any point (any local region) depends of the whole domain (of all mantle). Geologists also know many examples of coherence events in removed from each other regions. Explanation of this contradiction is that the complete solution of the mathematical problem is composed of homogeneous and inhomogeneous parts. Seismic tomography data allow (under additional assumptions on the viscosity) find only an inhomogeneous part of the solution. Homogeneous part of the solution satisfies the boundary conditions. In modern regional studies, based on the data of

seismic tomography, boundary effects usually just ignored, which is equivalent to discarding the homogeneous part of the solution. Therefore, the accuracy of results (predictions) remains uncertain. Conditions for the absence outer actions are valid only at the upper boundary of the mantle, whereas at the lower boundary of the region and on its lateral boundaries the forces, heat and mass fluxes in the general case are different from zero. To improve the accuracy of regional modeling may be offered some arrangements. The general recommendation is that to allocate the study region out of the mantle should be done on natural boundaries without cutting it into pieces. As the lower boundary of the computational domain is preferable to take a natural border between the upper and lower mantle. In this case, according to Kotelkin et al., (2011) the condition of impermeability for the convection will be most justified, and for the thermal problem we obtain the reliable condition that a temperature is equal the temperature of the endothermic phase transition. As the natural lateral boundaries of the mantle (on which no forces and fluxes are acting) should be regarded the boundary of the convective cells, ie mid-ocean ridges and subduction zones. Besides, there is uncertainty of geodynamic modeling

associated with well known fact that thermal convection admits a set of stationary solutions, in other words our modeling is ill-posed problem.

Therefore, for geodynamic simulation is desirable to use additional conditions of regularization. As the regularizing conditions may be used a seismic tomography data (Ismail-Zadeh et al., 2013) or geological data (Kotelkin et al., 2013). These recommendations were used in the study of thermal convection in an elongated upper mantle region, on the lateral boundaries of this region are supported ascending flows to simulate presence and action of mid-oceans ridges. The numerical 2D-modeling took into account changes in viscosity caused by temperature, phenomenon of solidus and exothermic phase transition at a depth of 410 km. Also was modeled the presence of lightweight crustal material over the mantle and was simulated his behavior. Dynamic visualization of calculations shows that a lightweight material forms a continent which is floating in the central part of region, and near the edges of the continent are functioning two active subduction zones. In this case, convection in the upper mantle has a clearly pronounced cyclical character. There is a phase during which is watching the oblique subduction of plates beneath the continent, and the continent at this time is stretched. When the space under continent will be filled by slabs, the convection rebuilds. Now is realizing another convective phase during which is watching the

vertical subduction with overturn of slabs and their movement in the inverse direction, at this time the continent is compressed. When switching modes of convection takes place known to geologists mysterious phenomenon when the background of the total extension there are local pieces with a compression and vice versa. Sea level is lowered when the continent is compressed and increases when the continent is elongated.

References

- Ismail-Zadeh, A., Honda, S., Tsepelev, I., 2013. Linking mantle upwelling with the lithosphere decent and the Japan Sea evolution: a hypothesis. *Scientific Reports*, 3, 1137. DOI:10.1038/srep01137
- Kotelkin, V.D., Lobkovskii, L.I., 2011. Thermochemical Theory of Geodynamical Evolution *Doklady Earth Sciences*. 438. 622–626. DOI: 10.1134/S1028334X11050333
- Kotelkin, V.D., Lobkovskii, L.I., 2013. Modeling of Regional Geodynamics Using Geological Data *Doklady Earth Sciences*. 450, 521–525. DOI: 10.1134/S1028334X13050048

The late Mesoproterozoic to late Palaeozoic evolution of Central Asia and comparison with the SW Pacific

A. Kröner^{a,b}, Y. Rojas-Agramonte^{a,b}

^aBeijing SHRIMP Centre, Institute of Geology, Chinese Academy of Geological Sciences, 26 Baiwanzhuang Road, 100037 Beijing, China, e-mail: kroener@uni-mainz.de

^bDepartment of Geosciences, University of Mainz, 55099 Mainz, Germany

The Central Asian Orogenic Belt (CAOB) occupies much of central and northeastern Asia and reflects a ca. 800 Ma history of accretion and collision from the latest Mesoproterozoic to late Palaeozoic. For most of its long history it consisted of a huge archipelago of island arcs and microcontinental fragments separated by numerous small ocean basins within a constantly changing large oceanic domain known as the Palaeo-Asian Ocean (PAO). We challenge the previous view that considered this extensive orogenic belt, named Altaids after Suess (1904), to have evolved from a single, long-lived arc system in the Palaeozoic, outboard of a large continental block consisting of the Baltic and Siberian cratons (Sengör et al., 1993).

The oldest record in the CAOB are latest Mesoproterozoic (ca. 1020-1050 Ma) ophiolitic remnants on the margin of the Siberian craton, followed southwards by continuously younger Neoproterozoic island arc systems, associated accretionary wedges and tectonically dismembered ophiolites. Continental fragments of Archaean to Neoproterozoic age, often exposing high-grade

metamorphic rocks, are wedged between these younger terranes and were the source of many Palaeozoic granitoid suites and xenocrystic as well as detrital zircons in arc-related volcanic and sedimentary assemblages. The assumption of a juvenile origin for most of the CAOB rocks, mainly based on the single-arc model, is erroneous as shown by a large number of Nd and Hf isotopic data that demonstrate extensive reworking of old crust during the orogeny and the presence of Precambrian subcrustal mantle lithosphere beneath the Palaeozoic assemblages.

Palaeomagnetic data demonstrate extensive terrane rotations during the accretionary process, making it very difficult, if not impossible, to reconstruct the palaeogeography within the PAO. Many of the Precambrian continental fragments and detrital zircons found in the Tianshan, Kazakhstan, Mongolia and southern Siberia are likely to be derived from the Tarim craton whose position in the Neoproterozoic was close to northwestern Australia in Gondwana. This is similar to the situation in Indonesia where

Australian crustal fragments and Australia-derived detrital and xenocrystic zircons are abundant (Hall and Sevastianova, 2012). Also, as in Indonesia, continental crust has arrived and drifted northwards in the PAO in multiple episodes, and has been fragmented and juxtaposed by subduction-related processes.

Other accretionary orogens such as the Tasmanides of eastern Australia (Glen, 2013) and SW Japan (Jahn, 2010) also show evidence of involvement of much old crust, and juvenile additions are less voluminous than previously assumed. The isotopic systematics of magmatic rocks in the CAOB, coupled with single-grain zircon dating, provide a record of heterogeneous crustal growth during the accretionary evolution of this huge orogenic domain (Kröner et al., 2014), and we suggest that the evolution of this huge orogenic domain mirrors the development of the present SW Pacific during the Jurassic to Present (e.g., Hall and Sevastianova, 2012).

References

- Glen, R., 2013. Refining accretionary orogen models for the Tasmanides of eastern Australia. *Australian Journal of Earth Sciences*
- Hall, R., Sevastjanova, I., 2012. Australian crust in Indonesia. *Journal of Australian Earth Sciences* 59, 827–844.
- Jahn, B.-M., 2010. Accretionary orogen and evolution of the Japanese islands—Implications from a Sr-Nd-isotopic study of the Phanerozoic granitoids from SW Japan. *American Journal of Science* 310, 1210–1249.
- Kröner, A., Kovach, V., Belousova, E., Hegner, E., Armstrong, R., Dolgopolova, A., Seltmann, R., Alexeiev, D.V., Hoffmann, J.E., Wong, J., Sun, M., Cai, K., Wang, T., Tong, Y., Wilde, S.A., Degtyarev, K.E., Rytsk, E., 2014. Reassessment of continental growth during the accretionary history of the Central Asian Orogenic Belt. *Gondwana Research*, 25, 103-125.
- Sengör, A.M.C., Natal'in, B.A., Burtman, V.S., 1993. Evolution of the Altaiid tectonic collage and Paleozoic crustal growth in Eurasia. *Nature* 364, 299–307.
- Suess, E., 1904. *The Face of the Earth (Das Antlitz der Erde)*, vol. 3, Clarendon Press, Oxford.

Seismic Evidence for Ancient Subduction of Izanagi Plate: Implications for Regional Mantle Viscosity

J. Li^{a,*}, D. A. Yuen^{b,c}

^aKey Laboratory of the Earth's Deep Interior, Institute of Geology and Geophysics, Chinese Academy of Sciences, 100029 Beijing, China

email: juanli@mail.igcas.ac.cn

^bSchool of Environment Sciences, China University of Geosciences, 430074 Wuhan, China

^cDepartment of Earth Sciences, University of Minnesota, Minneapolis, MN 55455, USA

Plate reconstruction studies have shown that Izanagi Plate is one of the most important tectonic units shaping the tectonic structure of East Asia from the Cretaceous to the Eocene (e.g. Sento et al., 2012; Whittaker et al., 2009). The absence of ocean floor of the subducted Izanagi plate and fragmented geochemical dataset has cast a doubt of the existence of this ancient plate, and when and how it subducted completely beneath East Asia. In this study, we found the seismic evidence for the remnant of ancient Izanagi plate which had subducted into the lower mantle. We undertook a systematic search for deep mantle heterogeneities beneath northeast China and the adjacent Japan Sea through S-to-P converted wave studies. Array stacking techniques were applied to detect the weak signature of the scattered waves indicative of the lower mantle structure. Broad mid-mantle scatterers with depths ranging from 930 to 1120 km were revealed to the east of the trapped stagnant

slab. We argue that the accumulation of MORB-like slab materials at mid-mantle depths causes a different chemical composition than that of the surrounding peridotitic mantle. The spatial isolation of the heterogeneities from the long westward-extending stagnant Pacific slab suggests an origin related to the subduction of ancient Izanagi plate. In combination with the reconstruction history of plate motions, we estimate the viscosity of the topmost lower mantle to vary from 1.0×10^{22} to 1.6×10^{23} Pa s, which in turn provides an additional constraint for unravelling of the dynamical processes and tectonic history under East Asia up to at least 50 Myr.

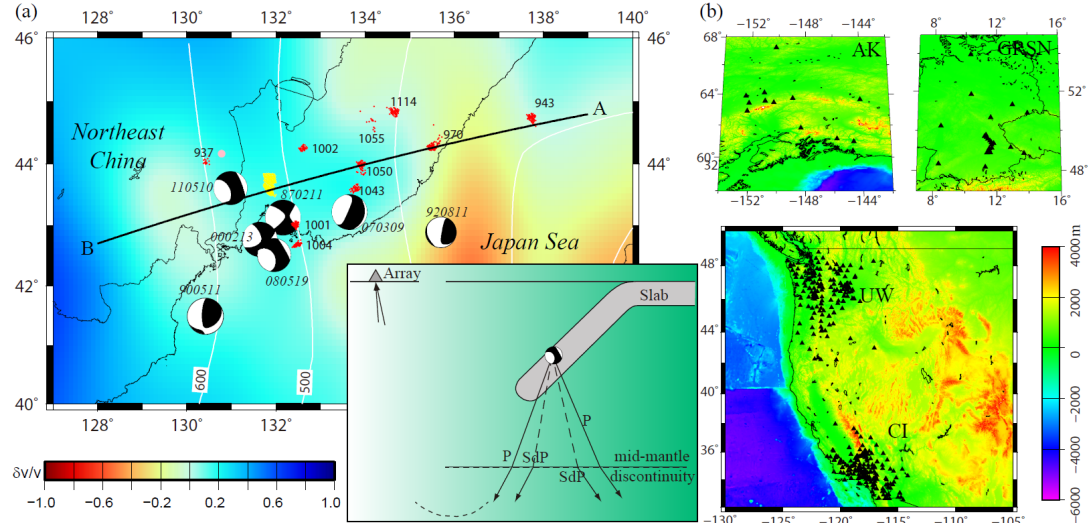


Figure 1 Location of the events investigated and the station distributions. (a) The large beachballs show the source mechanisms of the seven events with the $S_{1000}P$ phase observed. The red point clusters are the conversion points calculated at an assumed depth of 1000 km for the $S_{1000}P$ phase, and the adjacent numbers indicate the depths of the observed scatterers. The P velocity model (Fukao et al., 2001) for the depth range 900 to 1000 km is shown in the background. Line AB indicates the position of the cross-section shown in Figure 4. Yellow points indicate the conversion location of SdP phase of the Mw 6.9 earthquake analyzed by Niu (2013). (b) Distribution of seismic arrays; the triangles indicate the stations used. Insect is a schematic plot showing the ray paths of the P and SdP phases (Li and Yuen, 2014).

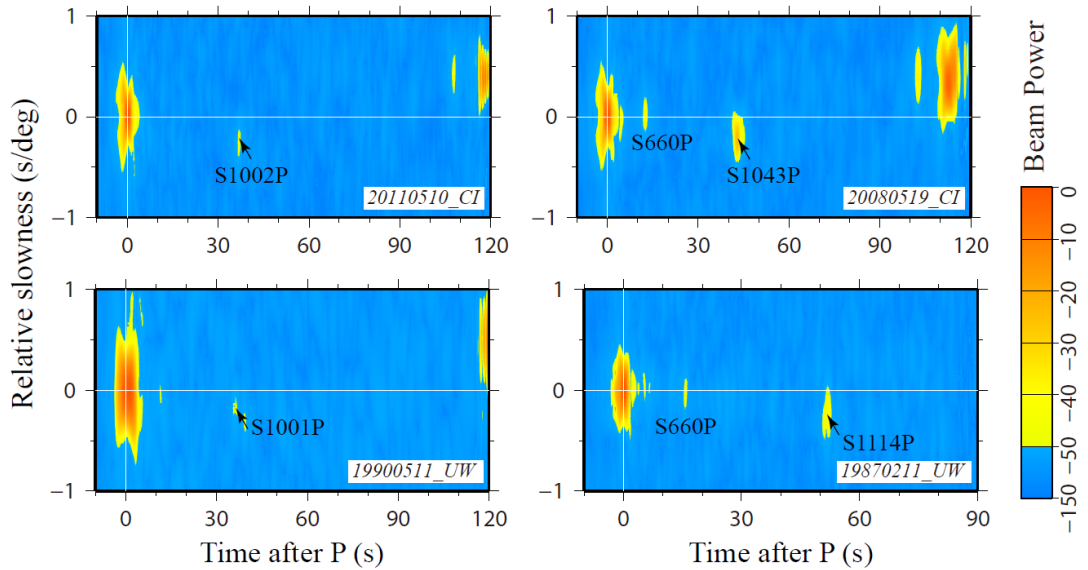


Figure 2 Examples showing stacked color contour map with the $S_{1000}P$ phase clearly identified. “Hotter” color clusters represent greater energy and indicate a phase arrival. $S_{1000}P$ arrivals, which are identified by the slowness and arrival time, are indicated by black arrows. The conversion phase at the 660-km discontinuity, where detectable, is marked (Li and Yuen, 2014).

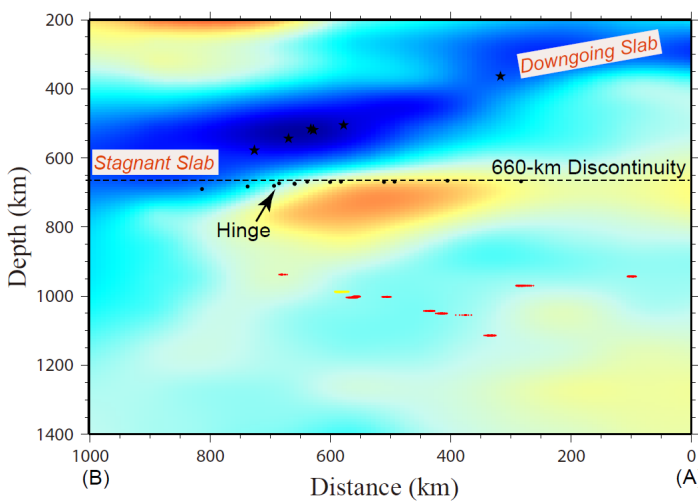


Figure 3 Depth cross section along line AB in Figure 1 with the conversion points of $S_{1000}P$ indicated by dense red dots. The depth section of the P wave velocity model (Fukao et al., 2001) is also plotted, with blue and red colors indicating fast and slow velocity anomalies. The black dots mark the undulation of the 660-km discontinuity investigated by S-to-P scattered wave (Li et al., 2008), and the rapid change of the 660-km discontinuity constrains the hinge of the slab.

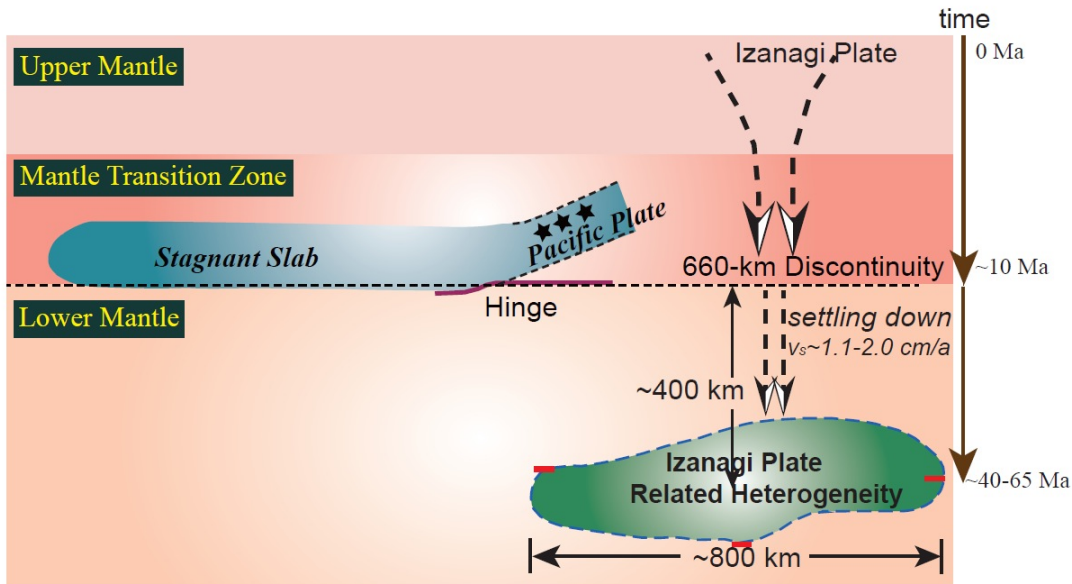


Figure 4 Schematic diagram showing the location of the mid-mantle heterogeneity, which might be related to the ancient Izanagi plate subduction. Time of transportation of Izanagi plate related anomalies from the surface to the observed depth can be estimated from history of plate reconstruction and our seismic observations. Assuming those scatterers (thick red bar) roughly constraining the spatial distribution of the heterogeneities, the viscosity of the topmost lower mantle beneath the study region can be estimated (Morra et al., 2010). The purple line is the topography of the 660-km discontinuity (Li et al., 2008) revealed by seismic scattered waves.

References

- Fukao, Y., Widjiantoro S., Obayashi M., 2001. Stagnant slabs in the upper and lower mantle transition region, *Reviews of Geophysics* 39(3), 291-323.

- Li, J., Chen, Q.F., Vanacore, E., Niu, F., 2008. Topography of the 660-km discontinuity beneath northeast China: Implications for a retrograde motion of the

- subducting Pacific slab, *Geophys Res. Lett.* 35 (1), L01302.
- Li, J., Yuen D., 2014. Mid-mantle heterogeneities associated with Izanagi plate: implications for regional mantle viscosity.
- Morra, G., Yuen, D., Boschi, L., Chatelain, P., Koumoutsakos P., Tackley, P. J., 2010. The fate of the slabs interacting with a density/viscosity hill in the mid-mantle. *Physics of the Earth and Planetary Interiors*, 180 (3–4), 271-282.
- Niu, F., 2013. Distinct compositional thin layers at mid-mantle depths beneath northeast China revealed by the USArray, *Earth and Planetary Science Letters*.
- Seton, M., et al., 2012. Global continental and ocean basin reconstructions since 200 Ma, *Earth-Science Reviews*, 113 (3–4), 212-270.
- Whittaker, J. M., Müller, R.D., Leitchenkov, G., Stagg, H., Sdrolias, M., Gaina, C., Goncharov, A., 2007. Major Australian-Antarctic Plate Reorganization at Hawaiian-Emperor Bend Time. *Science*, 318 (5847), 83-86.

Earthquakes, fluids, and climate - or: what controls orogeny in a forearc system?

O. Oncken

GFZ Potsdam, Telegrafenberg, D-14473 Potsdam, Germany, oncken@gfz-potsdam.de

Accumulation of deformation at convergent plate margins is recently identified to be highly discontinuous and transient in nature: silent slip events, non-volcanic tremors, afterslip, fault coupling and complex response patterns of the upper plate during a single as across several seismic cycles. Similarly, long-term accumulation of deformation at convergent plate margins is known to be equally variable, chiefly dominated by the principal style of mass flux: accretionary versus erosive. Increasing evidence is beginning to indicate that the long- and short-term processes show intriguing relationships. Segments of convergent plate margins with high recurrence rates and at different stages of the rupture cycle like the Chilean margin offer an exceptional opportunity to study these features and their interaction.

Major recent seismic events have occurred in south Central Chile and in Northern Chile or are expected in the very near future (Iquique, last ruptured 1877) allowing observation at critical time windows of the seismic cycle. The reflection seismic data exhibit well defined changes of reflectivity and Vp/Vs ratio along the plate interface that can be correlated with different parts of the coupling zone as well as with changes during the seismic cycle. Observations suggest an

important role of the hydraulic system, and of lateral variation of locking on subsequent rupture and aftershock distribution as evidenced by the recent Maule earthquake. Moreover, evidence from exhumed ancient portions of a seismogenic coupling zone in the European Alps clearly underlines the dominant role of the fluid system during the seismic cycle.

Finally, the response of the upper plate in terms of fault activation as well as vertical motion at various time scales appears to be strongly correlated with the distribution of properties at the plate interface. Coseismic and interseismic vertical displacement, in contrast exhibit contrasting modes in the same area. Hence, kinematics varies during a single seismic cycle, and: the dominant deformation observed within one seismic cycle contrasts with long term deformation as evidenced by topography and major structures. Analogue and numerical modelling lend additional support to the kinematic patterns linking slip at the seismogenic coupling zone and upper plate response in forearc systems. Finally we note that the characteristic peninsulas along the South American margin constitute stable rupture boundaries and appear to have done so for a protracted time as evidenced by their long-term uplift history since at

least the Late Pliocene that points to anomalous properties of the plate interface affecting the mode of strain accumulation and plate interface rupture.

In summary, the climatically-controlled sediment flux into the trench and the subduction channel as well as the associated hydraulic

properties of the latter and the overlying upper plate appear to be the dominating parameters affecting mass flux patterns and the response styles of the overlying plate.

The role of Serpentinite in lubricating Subduction Zones

T. Poulet^a, M. Veveakis^a, K. Regenauer-Lieb^{a,b}, D. A. Yuen^{c,d}

^aCSIRO Earth Science and Resource Engineering

^bThe University of Western Australia

^cMinnesota Supercomputer Institute, University of Minnesota

^dChinese University of Geosciences, Wuhan

During the last decade knowledge over Episodic Tremor and Slip (ETS) events has increased dramatically owing to the widespread installation of GPS and seismic networks. The most puzzling observations are: (i) the periodic nature of slow seismic events (ii) their localization at intermediate depths estimated (15-40 km), and (iii) the origin of the non-volcanic fluids that are responsible for the slow slip and resulting tremor activity. We reconcile these observations using a first principles approach relying on physics, continuum mechanics and chemistry of serpentinite in the megathrust interface. The approach reproduces the GPS sequences of 17 years of recording in Cascadia, North America, as well as over 10 years in the Hikurangi trench of New Zealand.

We show that strongly endothermic reactions, such as serpentinite dehydration, are required for ETS events.

We report that in this tectonic setting it is its chemical reaction kinetics, not the low friction, that marks serpentinite as a key mineral for stable, self-sustained oscillations.

We find that the subduction zone instabilities are driven from the ductile realm rather than the brittle cover. Even when earthquakes in the cover perturb the oscillator it relaxes to its fundamental mode. Such a transition from stable oscillations to chaos is witnessed in the ETS signal following the M 6.8, 2007 Gisborne event, which triggered a secondary mode of oscillations that lasted for a few years. As a consequence we postulate that the rich dynamics of ductile modes of failure may be used to decipher the chaotic time sequence underpinning seismic events.

Geology and setting of Viti Levu Island, Fiji

B. Rao

School of Geography, Earth Science and Environment, The University of the South Pacific, Laucala Campus, Suva, Fiji Islands, e-mail: raobhask@gmail.com

Viti Levu is the largest of the islands in the Fijian Archipelago and has a geological history dating back to the Eocene. The oldest rocks on the island are part of the Late Eocene to Early Oligocene Yavuna Group outcropping to the south and west of Nadi dated overlain unconformable and comprise an early or primitive arc sequence composed of submarine lavas, and minor intercalated sediments including limestone bodies intruded by a large tonalite body, the Yavuna Stock. These Yavuna Group rocks are unconformably overlain by a somewhat younger arc series, the Wainimala Group of Late Oligocene to Middle Miocene in age which overlie and generally skirt the Yavuna rocks to the south and form an arcuate band that stretches across Viti Levu into the adjacent Yasawa Island Group to the west. The folded axis of this younger volcanic arc is marked by a series of smaller and younger plutonic bodies (Colo Plutonics) ranging from gabbro to tonalite in composition and of Middle to Late Miocene age (12.5 to 7 Ma).

Emergence and erosion of the Oligocene-Miocene Wainimala volcano-plutonic arc resulted in deposition of coarse Wainimala and Colo derived sediments rocks initially to the south and east of the Yavuna Block (Tuva Group) and

within a group of strike slip basins in the Nadi (Nadi Sedimentary Group), Sovi (Navosa Group) and Navua Basins with deposition continuing into the Early Pliocene. This period also saw the emergence of calcalkaline volcanism on the island (Navosa Group, Namosi Andesite and other areas) whilst marine sedimentation in the south eastern part of the island led to the deposition of the Veisari Sandstone and the Suva Marl (Pliocene).

Much of the Pliocene volcanism on the island is restricted to the northern half of the island (the Koroimavua and Mba Volcanic Groups) and is decidedly shoshonitic in character with lesser amounts of calcalkaline and high-k calcalkaline volcanics. Some 15 eruptive centres are presently recognised and form a prominent NE-SW alignment. These volcanics are often hosts to significant epithermal gold-silver mineralisation.

Creep Fractures in the Mantle and their role for Deep Fluid Transfer

K. Regenauer-Lieb^{a,b}, M. Veveakis^b, T. Poulet^b, H. Sommer^c, A. Karrech^a, J. Liu^a, C. Schrank^a

^aThe University of Western Australia

^bCSIRO Earth Science and Resource Engineering

^cUniversity of the South Pacific, Fiji

^dQueensland University of Technology

When hot and ductile rocks fail they do so with an astonishing variety. Observations from crustal deformation show that when the fluid content is low (less than a few per cent) they form the cores of anastomosing mylonitic shear zones, which feature strong gradients in grain size towards their metamorphic fluid rich centre (Fusseis et al., 2009). In circumstances where the fluid/melt content is high they form macroscopically visible ductile fractures (Weinberg and Regenauer-Lieb, 2010) which allow melt transfer into the shallower crust forming the feeder zone of granites. We show here that all of the above phenomena are new types of instabilities well known from high temperature deformation of ceramics, i.e. materials that otherwise show brittle cleavage at cold laboratory conditions. The new failure modes boil down to a series of microscopic processes, where upon increasing temperature and decreasing applied stress failure modes transition from brittle cleavage to transgranular and intergranular “creep fractures”, summarized by Ashby’s classical deformation mechanism maps (Ghandi and Ashby, 1979).

Although Material Scientists are well aware of these creep enhanced fracture modes we have been lacking concise evidence in the laboratory and field proving the existence of these failure transitions. As creep fracture processes are happening on relatively slow geodynamic time scales they have been argued to provide the critical mechanism linking plate tectonic processes and deep fluid transfer processes (Regenauer-Lieb, 1999). In these considerations fluids are viewed as creating their own pathways through facilitating shear localization by creep fractures, rather than being a passive constituent simply following brittle fractures that are generated inside a shear zone caused by other localization mechanisms.

Recently, the missing laboratory (Rybacki et al., 2008) and field evidence for creep fractures have been found (Fusseis et al., 2009). Ghost images of both creep fractures and brittle fractures can also be seen in OH diffusion profiles on grain boundaries (Sommer et al., 2008) and fully embedded intragranular cracks in mantle xenoliths (Sommer et al., 2012).

In order to illustrate the fundamental implications for deep fluid transfer we extend classical solutions of material sciences to geodynamic conditions and incorporate melting reactions into the numerical formulation. We will show the implications to a number of applied field studies.

References

- Fusseis, F., Regenauer-Lieb, K., Liu, J., Hough, R.M., De Carlo, F., 2009. Creep Cavitation can establish a granular fluid pump through the middle crust *Nature*. 459, 974-977.
- Ghandi, C., M.F. Ashby, M.F., 1979. Overview No. 5 Fracture-Mechanism Maps for materials which cleave: F.C.C., B.C.C. and H.C.P. metals and ceramics. *Acta Metallurgica*. 27, 1565-1602.
- Regenauer-Lieb, K., 1979. Dilatant plasticity applied to Alpine Collision: ductile void growth in the intraplate area beneath the Eifel Volcanic Field. *Journal of Geodynamics*, 27, 1-21.
- Rybacki, E., Wirth, R., Dresen G., 2008. High-strain creep of feldspar rocks: Implications for cavitation and ductile failure in the lower crust *Geophysical Research Letters*. 35, L04304.
- Sommer, H., Regenauer-Lieb, K., Gasharova, B., Siret, D., 2008. Grain Boundaries: A possible water reservoir in the Earth Mantle? *Mineralogy and Petrology*, 94, 1-8.
- Sommer, H., H., Regenauer-Lieb, K., Gasharova, B., Jung, H., 2012. The formation of volcanic centers at the Colorado Plateau as a result of the passage of aqueous fluid through the oceanic lithosphere and the subcontinental mantle: New implications for the planetary water cycle in the western United States. *Journal of Geodynamics*. 61, 154-171.
- Weinberg, R., Regenauer-Lieb, K., 2010. Ductile Fracture and Magma Migration from Source. *Geology*, 38(4), 363-366.

The formation of micro diamonds in decompression cracks out of equilibrium controlled by the C:O:H ratio in the kimberlitic melt

H. Sommer^a, B. Gasharova^b, K. Regenauer-Lieb^{c,d}, W. Colliston^e, J. Potgieter^e

^aSchool of Geography, Earth Science and Environment, The University of the South Pacific, Laucala Campus, Suva, Fiji Islands, e-mail: info@holgersommer.de

^bANKA/Inst. Synchotron Radiation, Forschungszentrum Karlsruhe GmbH, Hermann-von-Helmholtz-Platz 1, Eggenstein-Leopoldshafen, D-76344 Germany

^cSchool of Earth & Geographical Sciences, The University of Western Australia, Perth, Western Australia 6009, Australia

^dCSIRO Exploration & Mining, PO Box 1130, Bentley, WA 6102, Australia

^eDepartment of Geology, University of the Free State, PO Box 339, Bloemfontein 9301, South Africa

Diamonds are supposed to be formed in the diamond window under high-pressure conditions due to the polymorph graphite/diamond phase transition. In this study we present for the first time, that natural diamonds can be formed by C:O:H bearing volatiles during the uplift of the kimberlitic melt in eclogites from the Roberts Victor mine, South Africa. Our results give evidence that the kimberlitic melt acts like a catalyst, and therefore the C:O:H ratio in the kimberlite changes through the uplift of the kimberlite permanently, caused by the formation of hydrous and carbonatitic minerals within the kimberlitic melt. This catalytic process leads to the growth of light carbon bearing molecules and under favorable thermodynamic, stoichiometric and kinetic conditions micro diamonds can be formed,

even under lower pressure conditions outside of the diamond window. High-spatial-resolution synchrotron based FT-IR has been used to detect C:O:H-bearing volatiles around planar defect structures in garnet. In micro diamond bearing planar defect structures, a correlation between C:O:H-bearing volatiles could be identified whereas in micro diamond free planar defect structures no correlation of the different C:O:H containing volatiles is visible. The conclusions from our study proves that C:O:H-bearing volatiles, and their distribution pattern around the studied micro cracks, are suggestive of the formation of micro diamonds in natural eclogites.

Petrography, petrology and mineralogy of eclogite nodules from the Jwaneng Diamond Mine, Botswana. An approach documented by mantle metasomatism, kimberlite emplacement and finally by super sonic uplift of the diamondiferous host rocks

H. Sommer^a, K. Regenauer-Lieb^{b,c}, O. Gaede^{b,d}, B. Gasharova^e

^aSchool of Geography, Earth Science and Environment, The University of the South Pacific, Laucala Campus, Suva, Fiji Islands e-mail: info@holgersommer.de

^bSchool of Earth & Environment, The University of Western Australia, Perth, Western Australia 6009, Australia

^cCSIRO Earth Science and Resource Engineering, PO Box 1130, Bentley, WA 6102, Australia

^dSchool of Earth, Environmental and Biological Sciences, Queensland University of Technology, Brisbane, QLD 4000, Australia

^eInstitute for Photon Science and Synchrotron Radiation (IPS), Karlsruhe Institute of Technology (KIT), P.O. Box 3640, 76021 Karlsruhe, Germany

Scientific contributions and therein geochemical datasets applied to mantle xenoliths collected from the Jwaneng Diamond Mine in Botswana are very rare, because of the problematic accessibility of the mine and additionally the strong alteration of the xenoliths nodules itself. In this study we present a unique and detailed petrographical, petrological and mineralogical dataset applied to these very extraordinary eclogite nodules from the Jwaneng Diamond Mine. Our results show, for the first time strong evidence for mantle metasomatism in the studied area and additionally we calculated the duration of the mantle metasomatic event, which last ~100 Ma, based on Mg diffusion profiles in garnet. Furthermore, the outcome of our survey show, that the investigated eclogite nodules, has been affected by a mixture of Group I and Group II kimberlites. The formation of Group I kimberlite was caused by the depleted mantle and the development of the later Group II kimberlite by the enriched mantle. The source of the enriched mantle

was probably from a megalith, a remnant of a former oceanic crust related to the eastward subduction from the Scotia arc during Jurassic eras. Emplacement of the later mica rich Group II kimberlite leads finally to the explosive eruption kinetics of the kimberlite and consequently to the supersonic uplift of the diamond bearing host rocks. At this point, our results indicates, that supersonic uplift from the Earth's mantle to the Earth's surface of the diamondiferous host rocks took place with an velocity of up to ~1200 km/h (333 m/s) after mantle metasomatism took place. This outcome is based on OH diffusion profiles around totally embedded cracks in garnet. We corroborate this high estimate through velocities expected from viscous laminar flow driven by the pressure gradient. We also evaluate the velocity given by the conversion of gravitational potential energy into kinetic energy, which gives an upper kinetic limit and implies high velocities through the drag coefficients needed to support the

dense diamond bearing rock fragment in the melt. This robust evidence for near-acoustic wave speed velocity challenges our understanding of the basic mechanisms that can generate deep and fast cracks within the Earth.

The inferred speed of extraction shows that extreme mechanisms must be at work, which potentially starts as a melt filled propagating elastic crack at depth and during ascent accelerates through bubble feedback into its final explosive state.

From Gabbro to Granulite and finally to Kyanite- and bimineralic Eclogite: A petrological, geochemical and mass balance approach to mantle eclogites

H. Sommer^a, D. Jacob^b

^aSchool of Geography, Earth Science and Environment, The University of the South Pacific, Laucala Campus, Suva, Fiji Islands, e-mail: info@holgersommer.de

^bDepartment of Earth and Planetary Science, Macquarie University, North Ryde, NSW 2109, Sydney, Australia, e-mail: dorrit.jacob@mq.edu.au

In this study, we present the phase transitions from gabbro into granulite and finally into kyanite-bearing and bimineralic eclogite. The investigated rock sample is a heterogeneous coexisting kyanite-bearing and bimineralic eclogite from the earth's mantle collected at the Roberts Victor Diamond mine in South Africa. Plagioclase of the former granulite reacted completely out under low H₂O activity (fH_2O) to form these kyanite- bearing and bimineralic eclogites. To quantify the phase transitions of the original gabbroic precursor, which was first metamorphosed under *H-T* granulite facies conditions followed by metamorphism under Earth's mantle conditions into both types of eclogite, a petrological, geochemical and a mass balance approach has been made. *i)* The results from our petrological approach show that Ca-rich garnet, which is coexistent with Ca-rich omphacite are the metastable phases from the original granulite in the kyanite-bearing relict while Mg-rich garnet, coexistent with Na-rich omphacite are the stable phases in the bimineralic eclogite part which took place at ~5.5 Gpa and ~1200°C. *ii)* Our geochemical results show a positive Eu anomaly in garnet from the kyanite-bearing

part, which indicates that the igneous precursor of the granulite was a gabbro, probably formed as oceanic crust. Most of the REE show an excellent correlation with the major elements of the rock forming minerals during the plagioclase-out reaction of the former granulite. The LREE in garnet are removed during the formation of the bimineralic eclogite due to liquefying of the anorthite component in plagioclase of the former granulite. Whereas the HREE are enriched in garnets in the bimineralic part of the eclogite compared to those in the kyanite zone, and correlate with the Mg-Ca exchange between both garnet populations. *iii)* The results from our mass balance approach indicate that garnet in bimineralic eclogite was formed by 0.925 mole garnet and 0.075 mole plagioclase of the former granulite precursor. Whereas omphacite in the bimineralic eclogite have been formed by 0.625 mole clinopyroxene and 0.375 mole plagioclase of the earlier granulite. Following bimineralic eclogite forming reaction was calculated from our mass balance approach: $0.625 \text{ Cpx} + 0.45 \text{ Plag} + 0.925 \text{ Grs} + 0.89 \text{ MgO} + 1.15 \text{ CO}_2 = 1 \text{ Pyp} + 1 \text{ Omph} + 0.04 \text{ Ky} + 1.15 \text{ Cc}$. The

excess of MgO during final eclogitization interpreted to be added during mantle metasomatism. And finally, our results show that only those parts of the former granulite show the formation of bimineralic eclogite where water had access to the rock. The formation of the kyanite bearing eclogite out of the former granulite is just considered by liquefying of the anorthite component in plagioclase under very low H₂O fugacity.

GPS Approach Detecting Tsunami Energy Scales in Real-Time for Early Warnings

Y. T. Song

Jet Propulsion Laboratory, Pasadena, California 91109, USA. E-mail: Tony.Song@jpl.nasa.gov

Most tsunami fatalities occur in near-field communities of earthquakes at offshore faults. Early warning is key for reducing the number of fatalities. Unfortunately an earthquake's magnitude, even can be determined precisely, often does not gauge the resulting tsunami power. Previous studies have demonstrated that real-time GPS stations along coastlines are able to detect seafloor motions due to big earthquakes [Blewitt et al. 2006], and that the detected seafloor displacements are able to determine tsunami energy and scales instantaneously [Song 2007] for early warnings.

Here we further verify the capability of our completing coastal GPS network in detecting recent tsunamis, such as the 2010 M8.8 Chilean earthquake and the 2011 M9.0 Tohoku-Oki earthquake induced tsunamis.

Our method focuses on estimating tsunami energy directly from seafloor motions because a tsunami's potential or scale. Since seafloor motions are the only source of a tsunami, their estimation directly relates to the mechanism that generates tsunamis; therefore, it is a proper way of identifying earthquakes that are capable of triggering tsunamis, while being able to discriminate

those particular earthquakes from false alarms.

Reference

- Song, Y.T., 2007. Detecting tsunami genesis and scales directly from coastal GPS stations, *Geophysical Research Letter*, 34, L19602, doi:10.1029/2007GL031681.
- Song, Y.T., Han, S.C., 2011. Satellite observations defying the long-held tsunami genesis theory, *D.L. Tang (ed.), Remote Sensing of the Changing Oceans*, DOI 10.1007/978-3-642-16541-2, Springer-Verlag Berlin Heidelberg.
- Song, Y.T., Fukumori, I., Shum, C. K., Yi, Y., 2012. Merging tsunamis of the 2011 Tohoku-Oki earthquake detected over the open ocean, *Geophysical Research Letter*, doi:10.1029/2011GL050767.
- Xu, Z., Song, Y.T., 2013. Combining the all-source Green's functions and the GPS-derived source for fast tsunami prediction – illustrated by the March 2011 Japan tsunami, *Journal of Atmosphere Oceanic Tech.*, jtechD1200201.

Multi-decadal regional sea level shifts in the Pacific over 1985-2008

Y. T. Song, J. H. Moon

Jet Propulsion Laboratory, Pasadena, California 91109, USA. e-mail: Tony.Song@jpl.nasa.gov

Over the past two decades, the sea level in the western Pacific rose up to three times faster than the global mean, while its counterpart in the eastern Pacific including U.S. west coast was nearly stationary or decreasing. It is puzzling how long this pattern of regional sea level changes has been gone and what is the dynamic cause. Combining recently reconstructed long-term sea level data products, upper-ocean measurements, and a non-Boussinesq ocean circulation model, we show that, for the first time,

the regional sea-level trends have undergone two shifts, during the mid-1970s and in the early 1990s, in a manner of accelerating on one side of the Pacific, but decelerating on the other side. The multidecadal regional sea-level shifts are the consequence of upper-ocean heat changes due to the Pacific Decadal Oscillation (PDO)-induced ocean circulations. It is further suggested that the stationary sea level along the U.S. West coast can flip into an upward trend as what had happened in the period of 1980s if the climate-induced wind pattern shifts in the Pacific.

Late Mesozoic Evolution of the back-arc basins of the Southeast China Block

L. Shu, J. Yao

School of Earth Sciences and Engineering, Nanjing University, Nanjing 210093, China E-mail:
lsshu@nju.edu.cn

We studied the geological features of Mesozoic basins that are widely distributed in the Southeast China Block (SECB in short), to better understand the Mesozoic tectonic evolution related to Pacific subduction. Three-types of back-arc extensional basin related to subduction of Pacific Ocean are distinguished according to their tectonic settings, includes the middle Jurassic rifting-graben, early Cretaceous volcanic faulted-depression and late Cretaceous-Paleogene redbed faulted-depression basins. The rifting-graben basins were filled by alkaline basalt and bimodal volcanic rocks dated at 180-160 Ma (U-Pb), the huge-scale volcanic faulted-depression basins are composed by the rhyolite dated at 150-110 Ma (a peak of 130 Ma), rhyolitic tuff and a little basalt associations, and the redbed faulted-depression basins are characterized by remarked red-purple color and red-colored conglomerate, sandstone, siltstone and mudstone that were intruded by small granitic or gabbro dykes dated at 100-90 Ma (SHRIMP U-Pb). The alkaline basalt and bimodal volcanic rocks in the middle Jurassic show their tholeiite (for basalt) and peraluminous (for rhyolite) geochemical features, revealing a within-continent rift

environment; the rhyolitic rocks in the early Cretaceous are of calc-alkaline volcanic series under the back-arc extensional setting. Wide development of red basin is perhaps a response to the rifting of East Asian margin since Late Cretaceous. These features suggest that development of basin in SECB connects closely with the geotectonic evolution of Pacific, and formation of basins was derived from Late Mesozoic continental crustal thinning due to a back-arc expansion followed by mantle upwelling. The modern outcrops of numerous granites and basins occur in a similar level, and the Late Mesozoic granitic bodies contact with the adjacent coeval basins by large normal faults, suggesting that the modern landforms between granites and basins were yielded by the Late Mesozoic back-arc extension. In Late Mesozoic, the Wuyi orogenic belt is a paleo-geographically separating unit, the Ganjiang fault zone behaves as the western boundary of Early Cretaceous volcanic rocks, and the Zhenghe-Dapu fault zone separates the SE-China Coastal volcanic-sedimentary zone and the Wuyi orogenic belt. We discussed the geodynamic mechanisms forming various basins that were controlled by the subduction of the Paleo-

Pacific plate, proposing a two-stage tectonic evolution.

References

- Deng, P., Shu, L.S., Yu, X.Q., Sun, Y., Wang, B., Tan, Z.Z., 2004. Early-Middle Jurassic Basins and Features of Volcanic rocks in the Western Fujian-Southern Jiangxi Region. *Acta Petrologica Sinica* 20(3), 521-532.
- Shu, L.S., Zhou, X.M., Deng, P., Wang, B., Jiang, S.Y., Yu, J.H., Zhao, X.X., 2009. Mesozoic tectonic evolution of the southeast china block: New insights from basin analysis. *Journal of Asian Earth Sciences* 34, 376-391.
- Wang, D.Z., Shu, L.S., 2012. Late Mesozoic basin and range tectonics and related igneous rock assemblages of Southeast China. *Geoscience Frontiers* 3(2), 109-124.
- Zhou, X.M., Sun, T., Shen, W.Z., Shu, L.S., Niu, Y.L., 2006. Petrogenesis of Mesozoic granitoids and volcanic rocks in South China: A response to tectonic evolution. *Episodes* 29(1), 26-33.

Basement nature of the Chinese and Mogolian Altai: Precambrian detrital zircons and interpretation

M. Sun^a, Y. Jiang^a, C. Yuan^b, G. Zhao^a, W. Xiao^d

^aDepartment of Earth Sciences and Shenzhen Institute of Research and Innovation, University of Hong Kong, Hong Kong, China e-mail: minsun@hku.hk

^bGuangzhou Institute of Geochemistry, Chinese Academy of Science, China

^dInstitute of Geology and Geophysics, Chinese Academy of Science, China

Paragneisses occur in the Chinese and Mongolian Altai areas, and they were previously regarded as Precambrian basement. However, recently reported detrital zircon ages are dominantly 465–542 Ma old, with $\epsilon\text{Hf(t)}$ values varying from –25 to +15, indicating that these rocks were deposited in the Early Paleozoic. Old detrital zircons do exist, a few cluster at 1.8–2.0 Ga and sparse ones yield discordant ages around 2.3–2.6 Ga. Those Precambrian zircons give negative $\epsilon\text{Hf(t)}$ values between 0 and –28. Some researchers invoke an unexposed Precambrian basement to interpret the source of these old zircons. Here we argue that the old sediments were possibly derived from the micro-continents and arc terranes in western Mongolia. The Precambrian zircons resemble those from old rocks preserved in the western Mongolia and its adjacent arc terranes. Therefore, we suggest these old zircons more likely represent the detritus recycled from there. The Chinese Altai possibly represents a Paleozoic active continental margin rifted away from an old continent, like the NE Japan. Moreover, information from the detrital zircons, combined with previous palaeomagnetic constraints, favors

northern India as the potential origin, from which a small micro-continent drifted northwards and incorporated into the CAOB in a time interval from the Neoproterozoic to Early Paleozoic. Accordingly, the crustal growth of the CAOB in western Mongolia and the Chinese Altai can be outlined by secular amalgamation of magmatic arcs around a Precambrian micro-continent.

The research is supported by Hong Kong Research Grant Council (HKU705311P and HKU704712P), National Science Foundation (41273048), and a HKU CRCG grant. The work is a contribution to IGCP 592 by the Joint Laboratory of Chemical Geodynamics between HKU and CAS (Guangzhou Institute of Geochemistry).

Porphyry deposits and oxidized magmas

W. Sun^{a*}, H. Li^a, R. Huang^b, X. Ding^b, M. Ling^b

^aCAS Key Laboratory of Mineralogy and Metallogeny, Guangzhou Institute of Geochemistry, Chinese Academy of Sciences, 511 Kehua Street, Wushan, Guangzhou 510640, China;

e-mail: weidongsun@gig.ac.cn

^bState Key Laboratory of Isotope Geochemistry, Guangzhou Institute of Geochemistry, Chinese Academy of Sciences, 511 Kehua Street, Wushan, Guangzhou 510640, China.

Porphyry deposits supply most of the world's Cu and Mo resources. More than 90 % of the porphyry deposits are found at convergent margins, especially above active subduction zones, with much fewer occurrences in post-collisional or other tectonic settings. Porphyry Cu-(Mo)-(Au) deposits are essentially magmatic hydrothermal systems, which are generally initiated by injection of oxidized magmas saturated with metal-rich aqueous fluids, i.e., the parental magmas need to be water- rich and oxidized with most of the sulfur appearing as sulfate. Sulfur is the most important geosolvent controlling the behavior of Cu and other chalcophile elements, i.e., there are high partition coefficients for Cu and other chalcophile elements between sulfide and silicate melts. A small amount of residual sulfide can hold a large amount of Cu. Therefore, it is essential to eliminate residual sulfide to achieve high Cu contents in magmas for the formation of porphyry deposits. The magic number of oxygen fugacity is $\log f\text{O}_2 > \text{FMQ} + 2$ (i.e., $\Delta\text{FMQ} + 2$), where FMQ is the fayalite-magnetite-quartz oxygen buffer. Sulfate is over 10 times more soluble than sulfide. Therefore, the solubility of sulfur strongly depends

on sulfur speciation which, in turn, depends on oxygen fugacities. Most sulfur in magmas is present as sulfate at oxygen fugacities higher than $\Delta\text{FMQ} + 2$. Correspondingly, the solubility of sulfur increases from ~1000 ppm up to >1 wt %. Oxidation promotes the destruction of sulfides in the magma source and thereby increases initial chalcophile element concentrations, forming sulfur-undersaturated magmas that can further assimilate sulfides during ascent. Copper, Mo and Au act as highly incompatible elements in sulfide-undersaturated magmas, leading to high chalcophile element concentrations in evolved magmas. The final porphyry mineralization is controlled by sulfate reduction, which is usually initiated by magnetite crystallization, accompanied by decreasing pH and correspondingly increasing oxidation potential of sulfate. Hematite forms once sulfate reduction lowers the pH down sufficiently, driving the oxidation potential of sulfate up to the hematite–magnetite oxygen fugacity (HM) buffer, which is $\sim \Delta\text{FMQ} + 4$. Given that ferrous iron is the most important reductant responsible for sulfate reduction during porphyry mineralization, the highest oxygen fugacity favorable

for porphyry mineralization is the HM buffer. In addition to the oxidation of ferrous iron during crystallization of magnetite and hematite, reducing wall rocks may also contribute to sulfate reduction and mineralization. Nevertheless, porphyry deposits are usually mineralized in the entire upper portion of the pluton, whereas interaction with country rocks is generally restricted near the interface, therefore assimilation of reducing sediments is not likely to be a popular decisive controlling process. Degassing of oxidized gases has also been proposed as a major process responsible for sulfate reduction. Degassing, however, is not the main process in porphyry mineralization that occurs at 2-4 km depths in the upper crust. Sulfide formed during sulfate reduction is efficiently scavenged by aqueous fluids that transport metals to shallower depths, i.e., to the top of the porphyry and superjacent wall rocks. According to traditional views, sulfide saturation and segregation during magma evolution is not favorable for porphyry Cu±Au±Mo deposits. This is the main difference between porphyry deposits and Ni-Cu sulfide deposits. Nevertheless, in areas with thick reducing sediments, e.g., western North America, sulfide may often become saturated and segregated early during magmas evolution, forming Cu-rich accumulations beneath plutons. These Cu-rich sulfides may evolve into porphyry mineralization or control the ore-forming process. The contribution depends heavily on oxidation, i.e. major contribution can only be

expected when sulfide accumulations are oxidized to sulfate, liberating chalcophile elements. Sulfate reduction and ferrous Fe oxidation form H⁺, which dramatically lowers the pH values of ore-forming fluids and causes pervasive alteration zones in porphyry Cu deposits. The amount of H⁺ released during mineralization and alkali contents in the porphyry together control the intensity of alteration. In principle, H₂ and also methane form during the final mineralization process of porphyry deposits but are mostly oxidized by ferric Fe during subsequent processes. Some of the reduced gases, however, may survive the highly oxidizing environment, escape from the system, and even become trapped in fluid inclusions. Therefore, small amounts of reduced gases in fluid inclusions cannot argue against the oxidized feature of the magmas. Reduced magmas are not favorable for porphyry mineralization. Reduced porphyry deposits so far reported are either just host rocks away from the causative porphyry or were reduced through assimilation of reducing components during emplacement.

Sea level trend in New Zealand over the last century

R. Tenzer^a, A. Fadil^b

^aInstitute of Geodesy and Geophysics, School of Geodesy and Geomatics, Wuhan University, 129

Luoyu Road, Wuhan, China

^bNational School of Surveying, University of Otago, 310 Castle Street, Dunedin, New Zealand

Investigations in long-term instrumental tidal records reveal that 20th century sea level along the coast of New Zealand is rising at 1.46 ± 0.10 mm/yr in agreement with the regional rates of South Australia and Tasmania, and comparable to the global rate of 1.70 ± 0.20 mm/yr. We extend the advanced altimeter-gauge approach of combining satellite altimetry and tide gauge data with constraint equations from long-term adjacent tide gauge records to assess its performance in open seas and to explore the impact of vertical land motion on the observed relative sea level. This approach has again proven to be a robust method with an accuracy of 0.4 mm/yr. While no clear sea level rise pattern can be inferred once the tide gauge apparent sea level trends are corrected for vertical land motions from GPS, the advanced altimeter-gauge and geological vertical rates are completely consistent and reveal three temporal phases of sea level rise marked by an increase from 1.46 ± 0.10 mm/yr to 1.72 ± 0.10 mm/yr during the period (1900 – 1936), followed by a decrease to 1.48 ± 0.10 mm/yr during the period (1936 - 1956), and a substantial increase to 2.60 ± 0.10 mm/yr during the period (1956 - 1975). In contrast, the 20th century

microfossil proxy records of absolute sea level rise display nearly twice the global sea level rise rate of 3.17 ± 0.30 mm/yr and 3.28 ± 0.45 mm/yr respectively once salt-marsh records are corrected using GPS and geological vertical rates. Differential auto-compaction is a possible explanation, which needs further investigation.

Keywords Altimeter-Gauge, GPS, New Zealand, Salt-Marsh, Sea Level Rise, Vertical Land Motion.

Signature of the ocean-floor spreading in marine gravity

R. Tenzer

Institute of Geodesy and Geophysics, School of Geodesy and Geomatics, Wuhan University, 129 Luoyu Road, Wuhan, China

The evidence of ocean-floor spreading was given from marine magnetic surveys and later independently verified from the age dating of ocean-floor rock samples and from seismic studies. Here we show that a signature of the ocean-floor spreading is detectable also in gravity field. This is demonstrated using gravity data, which are corrected for gravitational signals of the (ocean crust) anomalous density structures and the Moho geometry, while revealing major density structures within the oceanic lithosphere. The other evidence is given for the (lateral) oceanic lithosphere density changes which are estimated from available global gravity and crustal structure models based on solving the Vening-Meinesz Moritz inverse problem of isostasy. The relations between the ocean-floor spreading (i.e., oceanic lithosphere age), the oceanic lithosphere density and the respective refined gravity field are established by means of a logarithmic model.

The model provides an empirical estimate of the lateral oceanic lithosphere density increase with its age, while the depth-dependent density changes are described by existing models of thermal lithospheric cooling. More localized density variations along the spreading ridge axes and over hot spots are not taken into consideration. The application of a newly established model of gravity changes with the oceanic lithosphere age for an independent validation of the thermal (oceanic) lithosphere correction to the isostatic marine gravity data is proposed.

Keywords age of ocean floor, gravity, mantle lithosphere, mid-ocean ridge, Moho interface, subduction zone

On capabilities of modern gravimetric methods in studying dynamic magmatic systems

P. Vajda^a, I. Prutkin^b, J. Gottsmann^c, M. Bielik^{a,d}, V. Bezák^a, R. Tenzer^e, L. Brimich^a

^aGeophysical Institute, Slovak Academy of Sciences, Bratislava, Slovakia, Europe,
 Peter.Vajda@savba.sk

^bInstitute of Geosciences, Jena University, Burgweg 11, D-07749 Jena, Germany

^cDepartment of Earth Sciences, University of Bristol, Bristol, UK

^dDepartment of Applied and Environmental Geophysics, Comenius University in Bratislava, Slovakia

^eSchool of Geodesy and Geomatics, Wuhan University, Wuhan, China

We present an inversion methodology by, which potential field data can be interpreted in structural or geodynamic studies. The method consists of several steps: removal of regional trend, depth-wise separation of signal of sources, line segments approximation of sources, and inversion by the method of local corrections yielding star-convex homogenous source bodies and/or contrasting contact surfaces. First we demonstrate a static application of the methodology on a case study devoted to identifying an intrusion

in structural tectono-geological investigation in the area of the Kolárovo gravity and magnetic anomalies of the Danube Basin in the Western Carpathian–Pannonian region of Central Europe. Next we demonstrate the capabilities of the methodology in geodynamic studies when studying the movement of magma/hydrothermal fluids in restless volcanic areas on a case of the 2004 unrest of Teide volcano, Tenerife, Canary Islands (Ablay et al., 2000; Andujar et al., 2010).

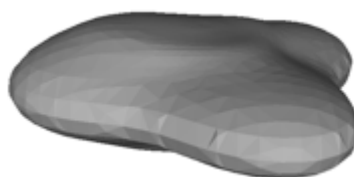


Fig. 1. Solution B.

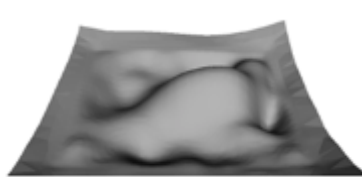


Fig. 2. Solution C

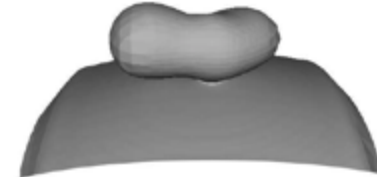


Fig. 3. Solution D

The presented inversion methodology produces a set of several admissible solutions that all are equally admissible from the viewpoint of observed gravity (and/or magnetic) data. Using additional geoscientific constraints or cognition, these solutions can be discriminated in terms of their geologic or tectonic feasibility. In the case of the Kolárovo gravity

and magnetic anomalies the following solutions are obtained: a single ellipsoidal intrusion below a sedimentary basin with determined morphology of its lower boundary, a single intrusion of a complex shape (solution B, Fig. 1), an uplift of the lower crust (solution C, Fig. 2), and an intrusion above uplifted lower crust (solution D, Fig. 3). Joint inversion of magnetic

and gravity data gives insights into magnetic properties of the intrusive

body.

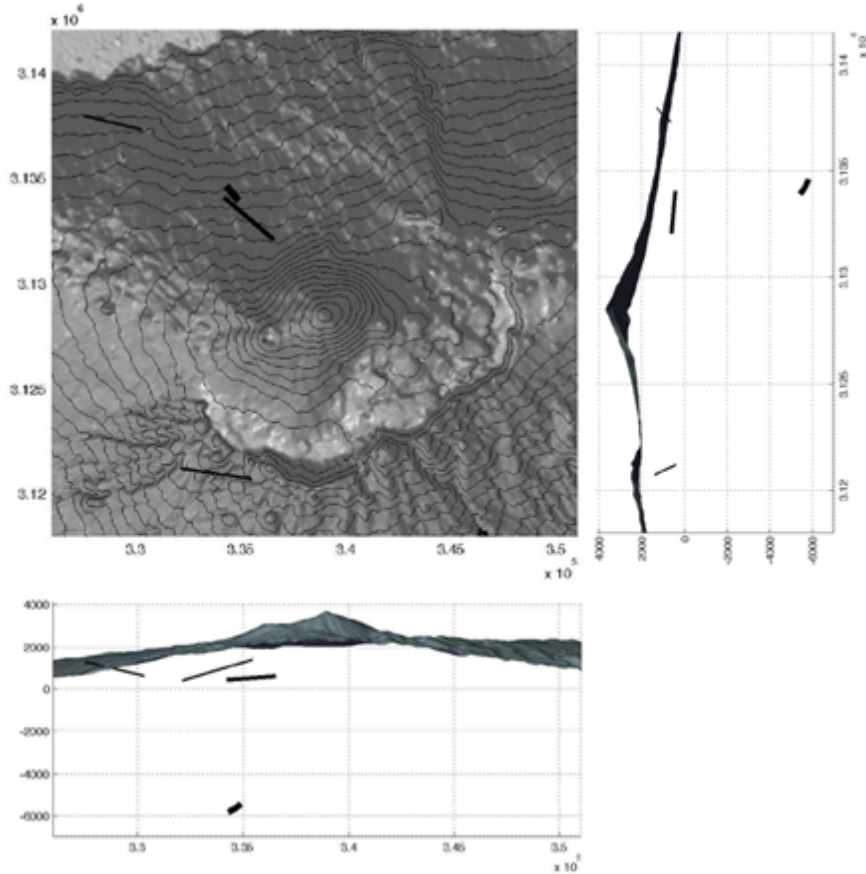


Figure 4.

The source line segments upon decomposition into shallow and deep sources. Top left plot is plan view, right plot is S–N cross-section, and bottom plot is W–E cross-section.

Next we proceed with geodynamic application of our gravimetric inversion methodology. During the seismic unrest at the central volcanic complex (CVC) on Tenerife bulk gravity increase was recorded across a network at the CVC between May 2004 and July 2005 (Gottsmann et al., 2006). Here we aim at interpreting the gravity signal in terms of multiple sources using a non-linear inversion based on line segments approximation. Residual gravity changes obtained by removing a trend were best-fitted with the

gravitational effect of 3 line segments (Vajda et al., 2012; Fletcher and Powell, 1963) that are located at depths 0–2 km b.s.l. We suspect that these line segments are composite sources representing shallower hydrothermal fluids and deeper magma injection. To test this hypothesis, we separate these composite sources vertically into shallow and deep sources by decomposing the residual gravity changes into “shallow-” and “deep-” fields while inverting both separately. The division level of 4

km below sea level (b.s.l.) was chosen to match roughly the upper boundary of the two seismogenic zones of (Cerdeña and del Fresno, 2011). The decomposition procedure, based on stepwise upward, downward and upward sequential harmonic continuations, is described in (Prutkin et al., 2011). The shallow and deep line segments obtained by the inversion are shown in Fig. 4.

Due to the spatial distribution of the shallow segments and the position of the deep one, as well as their spatial correlation with the seismogenic zones of (Cerdeña and del Fresno, 2011), we interpret the shallow segments as sources of hydrothermal fluids, while the short deep segment as a magma injection at a depth of about 6 km, within the NW zone of VT events swarm identified by (Cerdeña and del Fresno, 2011). This hybrid nature of the observed unrest is best explained by the migration of hydrothermafluids as a result of magma injection. The time span in-between the last three historic eruptions is roughly a century (93 and 111 years, respectively). Conspicuously enough, the 2004 unrest follows a similar repeatability pattern (95 years after Chinyero). We may consider the 2004 hybrid unrest on Tenerife a failed eruption.

Acknowledgements

Jo Gottsmann acknowledges support by the Royal Society University Research Fellowship and EC FP7 project “VUELCO” (grant # 282759). Peter Vajda was supported by the Slovak Research and Development Agency (contract No. APVV-0724-11) and by Vega

grant agency (projects No. 2/0067/12 and 1/0095/12).

References

- Ablay, G.J., Martí J., 2000. Stratigraphy, structure, and volcanic evolution of the Pico Teide – Pico Viejo formation, Tenerife, Canary Islands, *Journal of Volcanology and Geothermal Research*, 103(1–4), 175–208.
- Andújar, J., Costa, F., Martí, J., 2010. Magma storage conditions of the last eruption of Teide volcano (Canary Islands, Spain). *Bulletin of Volcanology* 72, 381–395.
- Cerdeña D.I., del Fresno C., Rivera L., 2011. New insight on the increasing seismicity during Tenerife's 2004 volcanic reactivation. *Journal of Volcanology and Geothermal Research* 206, 15–29.
- Fletcher R., Powell, M.J.D., 1963. A rapidly convergent descent method for minimization. *The Computer Journal* 6(2): 163–168.
- Gottsmann, J., Wooller, L., Martí, J., Fernández, J., Camacho, A.G., Gonzalez, P.J., Garcia, A., Rymer, H., 2006. New evidence for the reawakening of Teide volcano. *Geophysical Research Letters*, 33, L20311.
- Prutkin I., Vajda P., Tenzer R., Bielik, M., 2011. 3D inversion of gravity data by separation of sources and the method of local corrections: Kolarovo gravity high case study. *Journal of Applied Geophysics* 75(3), 472–478.
- Vajda P., Prutkin I., Tenzer R., Jentzsch G., 2012. Inversion of temporal gravity changes by the method of local corrections: A case study from Mayon volcano,

Philippines. Journal of
Volcanology and Geothermal
Research. 241–242, 13–20.

Tectonic of accretionary wedges response to variation of incoming plate variations along Manila Trench

S. Wu^a, C. Chen^{a,b}

^aKey Laboratory of Marine Geology & Environment, Institute of Oceanology, Chinese Academy of Sciences

^bUniversity of Chinese Academy of Sciences

The style of overriding plate deformation along northern Manila Trench is complex due to its geological setting, which is related to two distinctively tectonic processes: the initial arc-continent collision at southeastern Taiwan Island and the continent rifting at northern South China Sea (SCS). According to the differences of the sediment thickness, basement topography, water content and volcanic activity of the incoming crust, which are revealed by the newly integrated multi-beam and seismic data and the reprocessed seismic line 973, we suggest that the incoming crust along northern Manila Trench can be divided into three areas from north to south: Area A) the trapped oceanic crust with thick sediment and high pore pressure; Area B) transitional crust with thin sediment and widespread volcanic intrusion; Area C) normal SCS crust with relatively thick sediment. This incoming plate variation results in special style of deformation along the accretionary wedge, including the formation of a weak deformation belt, the reentrant trench geometry and the huge uplift of the upper slope. Area B may also give rise to profound change in the geometry of the subducted slab and the seismicity of seismogenic structures.

Keywords Manila Trench, accretionary wedge, incoming plate, seismic imaging

Mesozoic subduction history of the Paleo-Pacific plate beneath the Eurasian continent: Evidence from volcanic rocks in NE China

W-L. Xu*, F. Wang, F-P. Pei, H. Feng

College of Earth Sciences, Jilin University, Changchun 130061, China; e-mail: xuwl@jlu.edu.cn

When did the subduction of the Paleo-Pacific plate beneath the Eurasian continent begin (Wu et al., 2007)? How many times did its subduction happen during Mesozoic (Xu et al., 2013)? These issues have been unsolved. However, the spatial-temporal distributions of the Mesozoic volcanic rocks in NE China provide insights on these questions. Zircon U-Pb dating results indicate that the Mesozoic volcanisms in the eastern part of NE China can be subdivided into the following stages: 201-228 Ma, 174-190 Ma, 106-133 Ma, and 85-97 Ma (Xu et al., 2013). Late Triassic (201-228 Ma) volcanic rocks mainly occur in eastern Heilongjiang-Jilin provinces and are similar chemically to A-type rhyolite in the western margin of the Khanka Massif and bimodal volcanic rock association in the Lesser Xing'an-Zhangguangcai Ranges, implying an extensional environment after the final closure of the Paleo-Asiatic Ocean. Early-Middle Jurassic (174-190 Ma) volcanism is mainly distributed in the eastern Heilongjiang-Jilin provinces and consists of a calc-alkaline series within the continental margin (i.e., western margin of the Khanka Massif and a bimodal volcanic rocks in the Lesser Xing'an-Zhangguangcai Ranges, implying the beginning of the subduction of the Paleo-Pacific

plate beneath the Eurasian continent. Late-Early Cretaceous (106-133 Ma) volcanic rocks widely occur in NE China, and consist chemically of calc-alkaline series in the continental margin (i.e., eastern Heilongjiang-Jilin provinces) and bimodal rock association within intracontinent (i.e., the Songliao basin and the Great Xing'an Range), implying another westward subduction of the Paleo-Pacific plate beneath the Eurasian continent. Late Cretaceous (85-97 Ma) volcanic rocks only occur within the Songliao basin and the eastern margin of the Eurasian continent, the former is composed mainly of alkali basalts, the latter is made of a low- to middle-K calc-alkaline volcanic rocks, implying that they formed under the subduction of the Paleo-Pacific plate beneath the Eurasian continent. However, the Middle-Late Jurassic (155-166 Ma) and early Early Cretaceous (139-145 Ma) volcanic rocks in NE China only occur in the Great Xing'an Range and northern Hebei-western Liaoning provinces, belong chemically to high-K calc-alkaline series and A-type rhyolites, respectively. Combined with the regional unconformity in northern Hebei-western Liaoning provinces, we conclude that their formations should be related to the evolution of the Mongol-Okhotsk suture belt.

Therefore, we conclude: 1) the beginning of the subduction of the Paleo-Pacific plate beneath the Eurasian continent happened in Early Jurassic; 2) at least three times of subductions of the Paleo-Pacific plate beneath the Eurasian continent occurred during Mesozoic, i.e., Early Jurassic, late Early Cretaceous, and Late Cretaceous.

This work is supported by the NSFC (41330206 and 41272077).

References

- Wu, F.Y., Yang, J.H., Lo, C.H., Wilde, S.A., Sun, D.Y., Jahn, B.M., 2007. The Heilongjiang Group: a Jurassic accretionary complex in the Jiamusi Massif at the western Pacific margin of northeastern China. *The Island Arc* 16, 156–172.
- Xu, W.L., Pei, F.P., Wang, F., Meng, E., Ji, W.Q., Yang, D.B., Wang, W., 2013. Spatial-temporal relationships of Mesozoic volcanic rocks in NE China: constraints on tectonic overprinting and transformations between multiple tectonic systems. *Journal of Asian Earth Sciences* 74, 167–193.

Changes in local weather after 2004 Indian Ocean tsunami

Z. Y. D. Tang*

Research Center for Remote Sensing of Marine Ecology and Environment (RSMEE), State Key Laboratory of Tropical Oceanography, South China Sea Institute of Oceanology, Chinese Academy of Sciences, 164 West Xingang Road, Guangzhou 510301, PR China; e-mail: lingzistd@126.com

The present study analyzed the disturbance of the tsunami on local weather in Bay of Bengal (BoB) after the 2004 Indian Ocean Tsunami. After the tsunami, the local accumulated rainfall showed a notably increase (600 mm) in January of 2005 in the south east offshore of Sri Lanka (SES), and this increase was combined with evident decrease in sea surface temperature (SST) (up to -2°C) and increase in chlorophyll (up to 0.15 mg m⁻³). Four days averaged SST anomalies indicated a significant increase (1-4°C) shortly (Dec26 to Dec29, 2004) after the tsunami in south west of the epicenter (SWE).

Series of ocean atmospheric or biological variables changed successively after the change of SST, and the initial driving force was suggested from the tsunami. The chain of causality between the tsunami and the local weather changes is still unclear which calls for more direct studies.

Keywords Indian Ocean, tsunami, SST, rain, wind

Neoproterozoic Pacific type trench-arc system in the Jiangnan Orogen belt, South China: some important traces from rock assemblages, zircon U-Pb dating, Hf isotopes and whole rock geochemistry

J. Yao, L. Shu*

School of Earth Sciences and Engineering, Nanjing University, Nanjing 210093, China; e-mail:
lschu@nju.edu.cn

The Jiangnan orogenic belt is considered as the trace of the collisional suture zone between the Yangtze and Cathaysia blocks in South China. We investigate the mafic-ultramafic suites of Iherzolite, pyroxenite, gabbro, basalt and gabbroic diorite as well as red jasper interbedded with marine marbles that are exposed in the Yuanbaoshan domain of the western Jiangnan belt along the Neoproterozoic Shaoxing-Pingxiang-Shuangpai suture zone. The post-collisional granite plutons that intruded the ultramafic-mafic rocks are also found. Herewith, we present new zircon U-Pb data, Hf isotopes and related-whole rock geochemistry. Zircons in the gabbro yield a mean U-Pb age of 855 ± 5 Ma, whereas those from the granites show ages of 823 ± 5 , 831 ± 5 , 824 ± 5 and 833 ± 6 Ma. The Neoproterozoic mafic rocks display dominantly tholeiitic features and are characterized by negative Nb, Ta, Ba, Zr, Hf and Sr anomalies and LREE enriched patterns, with a minor negative Eu anomaly. The pyroxene-bearing diorite also exhibits similar geochemical characters. These features suggest that the mafic-ultramafic associations have a distinctive arc affinity. The zircons from the

gabbro show positive ϵ Hf(t) values ranging from 3.9 to 13.8. The granitoids are typical S-type granites with high ACNK values (1.15–1.40), and are classified as collision-related granites in tectonic discrimination diagrams. The zircons from these rocks show negative ϵ Hf(t) values of –18.99 to –0.84. We correlate the granitoids with the continent–continent collisional orogeny between the Yangtze and Cathaysia blocks. New results suggest a ~ 854 Ma arc setting occurred in the Yuanboashan domain and a fore-arc setting, in the SE-Yuanboashan, followed by an 840–820 Ma collisional process. This is different from previous proposals of the Neoproterozoic plume and bimodal magmatic settings dated around 830 Ma both in the Yangtze and Cathaysia Blocks.

References

- Shu, L.S., Charvet, J., 1996. Kinematics and geochronology of the Proterozoic Dongxiang - Shexian ductile shear zone: with HP metamorphism and ophiolitic melange (Jiangnan region, South China). Tectonophysics 267, 291–302.
Shu, L.S., 2012. An analysis of principal features of tectonic

- evolution in South China Block. Geological Bulletin of China 31(7), 1035–1053.
- Yao, J., Shu, L.S., Santosh, M., Li, J.Y., 2012. Geochronology and Hf isotope of detrital zircons from Precambrian sequences in the eastern Jiangnan Orogen: Constraining the assembly of Yangtze and Cathaysia Blocks in South China. Journal of Asian Earth Sciences 74, 225–243.
- Zhou, J.C., Wang, X.L., Qiu, J.S., Gao, J.F., 2004. Geochemistry of Meso- and Neoproterozoic mafic-ultramafic rocks from northern Guangxi, China: arc or plume magmatism? Geochemical Journal 38, 139–152.

Episodic widespread magma underplating in the Phanerozoic: Implication for craton destruction

H-F. Zhang

Department of Geology, Northwest University, Xi'an 710069, China
Institute of Geology and Geophysics, Chinese Academy of Sciences, Beijing 100029, China

Episodic widespread magma underplating into the ancient lower crust during Phanerozoic has been identified throughout the North China Craton (NCC) from early Paleozoic to Cenozoic, broadly corresponding to the Caledonian, Hercynian, Indosinian, Yanshanian, and Himalayan orogenies on the circum-craton mobile belts. The early Paleozoic ages come from xenoliths in the northern and southern margins, which mark the first phase of Phanerozoic magma underplating since the final cratonization of the NCC in the Paleoproterozoic. The magmatism coincided with the northward subduction of the Paleotethysian Ocean in the south and the southward subduction of the Paleoasian Ocean in the north. The subduction not only triggered magma underplating but also led to the emplacement of the diamondiferous kimberlites on the craton, marking the initiation of decrattonization. The late Paleozoic event as represented by the 315 Ma garnet pyroxenite and/or lherzolite xenoliths in Hannuoba was restricted to the northern and southern margins of the craton, correlating with the arc magmatism continuous associated with the subduction of the Paleotethysian and Paleoasian Oceans and resulting in the interaction between the melts from subducted slabs and

the lithospheric mantle/lower crust. The early Mesozoic event also dominantly occurred in the northern and southern margins and was related with the final closure of the Paleotethysian and Paleoasian Oceans as well as the collisional orogeny between the NCC and the Yangtze Craton. The late Mesozoic (120 Ma) was a major and widespread magmatic event which manifested throughout the NCC, associated with the geothermal overturn due to the giant south Pacific mantle plume. The Cenozoic magmatism, identified only in the dark clinopyroxenite xenoliths in the Hannuoba, was probably induced by the Himalayan movement in eastern Asia and might also have been influenced by the subduction of the Pacific Ocean to some extent. These widespread and episodic magma underplating or rejuvenation of the ancient lower crust beneath the NCC revealed by U-Pb and Hf isotope data resulted from the corresponding addition of juvenile materials from mantle to lower crust, with a mixing of the old crust with melts. The process inevitably resulted in the compositional modification of the ancient lower crust, similar to the compositional transformation from the refractory lithospheric mantle to a fertile one through the refractory peridotite – infiltrated melt reaction

as revealed in the lithospheric mantle beneath the craton.

Late Mesozoic giant magmatism in NE China and its adjacent region: Spatial-temporal variation and its tectonic significance

F-Q. Zhang^{a,b}, H-L. Chen^{a,b}, S-F. Yang^{a,b}, T-Y. Shao^{a,b}, M-N. A^{a,b}, K-F. Zhang^{a,b}, D-X. Chen^{a,b}, B. Deng^{a,b}, G. E. Batt^c, Q-A. Meng^d, J-P. Liang^d, Z-Z. Wang^d

^aDepartment of Earth Sciences, Zhejiang University, Hangzhou, China

^bStructural Research Center of Oil & Gas Bearing Basin of Ministry of Education, Hangzhou, China

^cThe Centre for Exploration Targeting, University of Western Australia, Australia

^dResearch Institute of Petroleum Exploration and Development, Daqing Oil Field, China

e-mail: zhangfq78@zju.edu.cn

Late Mesozoic igneous rocks are widespread in NE China. However, the origin of this large igneous province remains hotly debatable. The spatial-temporal variation framework of the Mesozoic igneous rock of NE China and its adjacent region has been proposed based on the new geochronological and geochemical data from the Hailaer basin of China, together with other available data from documents. The Late Mesozoic large scale magmatism in NE China lasted for more than 120 Ma since Jurassic and can be subdivided into four main stages: Early-Middle Jurassic (200-165Ma), Late Jurassic-early Early Cretaceous (165-150 Ma), late Early Cretaceous (135-100) and Late Cretaceous (95-80 Ma). Early-Middle Jurassic magmatism was dominated by granitic intrusion. Two opposite age-younging trends have been identified both from western and eastern continental margins toward hinterland of NE China, which indicated that the block of NE China was possibly controlled by two shallow subduction systems, Mongol-Okhotsk in the west and paleo-Pacific in the east. The Late Jurassic and early Early Cretaceous volcanic rocks mainly occurred in the Erguna Massif and

the Great Xing'an Range, where the volcanic rocks are bimodal, implying that they formed in an extensional environment after the final closure of the Mongol-Okhotsk Ocean. The late Early Cretaceous igneous rocks flared from the Great Xing'an Range in NE China and migrated progressively eastward. The rock types are various but dominant with acidic. Most of acidic rocks belong chemically to high-K calc-alkaline series and A-type rhyolite respectively. Combined with the regional unconformity and thrust structures in the Hailaer and Mohe basins, we suggest that these volcanics formed under a tectonic transition from a post-orogenic extension of the Mongol-Okhotsk orogeny to a back arc extension related to flat-slab foundering of the paleo-Pacific. The Late Cretaceous magmatic rocks, only distributed in the eastern Heilongjiang-Jilin provinces in NE China, mainly consist of low-K calc-alkaline andesitic rocks in the eastern Heilongjiang-Jilin provinces, indicated that a normal subduction of the Paleo-Pacific Plate occurred beneath the Eurasian continent.

Acknowledgement

This work was financially supported by National Natural Science Foundation of China (Grant No. 41272231, 41330207) and the National Science and Technology Major Project Program of China (Grant No. 2011ZX05009-001).

Jiangnan Orogen in South China: developed from divergent double subduction?

G. Zhao

Department of Earth Sciences, The University of Hong Kong, Pokfulam Road, Hong Kong

The Jiangnan Orogen is considered as a continent-continent collisional belt resulting from the closure of a Meso-Neoproterozoic ocean separating the southeastern margin of the Yangtze Block from the northwestern margin of the Cathaysia Block. Recent data indicate the existence of early Neoproterozoic (1000-825 Ma) volcanic arc assemblages on both sides of the orogen, suggesting that the ocean lithosphere between the Yangtze and Cathaysia blocks must have undergone divergent double-sided subduction during the period of 1000-825 Ma, like what is happening in the Moluccan ocean plate within the Pacific Ocean. The divergent double subduction eventually resulted in the closure of the ocean basin at ~825 Ma,

leading to the soft collision of the Yangtze and Cathaysia blocks to form the Jiangnan Orogen, without involvement of continental deep subduction, high-grade metamorphism of continental crust and uplift/exhumation of high-grade metamorphic rocks. Shortly after the collision, the initial detachment of the ocean lithosphere from the overlying crust and sedimentary sections induced underplating of mantle magmas, triggering partial melting of accretionary-wedge strata to form some peraluminous (S-type) granites in the period 825-815 Ma. Finally, the sinking of the oceanic slab pulled down the overlying strata to form some basins in which the Banxi Group and its equivalent strata including bimodal volcanic rocks were formed in the period 815-750 Ma.

